

DIFFERENTIATION OF HEALTHY AND CANCEROUS RENAL CELLS USING
SURFACE-ENHANCED RAMAN SCATTERING



by
Sevda Mert

Submitted to the Institute of Graduate Studies in
Science and Engineering in partial fulfillment of
the requirements for the degree of
Master of Science
in
Biotechnology

Yeditepe University

2013

DIFFERENTIATING OF HEALTHY AND CANCEROUS RENAL CELLS USING
SURFACE ENHANCED RAMAN SCATTERING

APPROVED BY:

Prof. Dr. Mustafa CULHA
(Thesis Supervisor)



Asst. Prof. Andrew HARVEY



Asst. Prof. Kaan KECECI



DATE OF APPROVAL: / /

ACKNOWLEDGEMENTS

First of all, I would like to express my deep gratitude to my advisor, Prof. Mustafa Culha, for his support, guidance, advice and especially great patience during my master program.

I would like to express my great appreciation to Yeditepe University Nanobiotechnology Group Members, Esen Efeođlu, Ertuđ Avcı, Mine Altunbek, Zehra Yılmaz, Seda Keleştemur, Manolya Hatipođlu, Şaban Kalay, Sinan Sabuncu, İbrahim Can Sevim, Cansu UmranTaş and Pınar Akkuş for their support and advice during my thesis.

I also would like to thank Asst. Prof. Dilek Telci for providing the cell lines used in the study. Also, I would like to thank to Ayca Zeynep Ilter for her support and suggestion about healthy and cancer cell lines.

Finally, I would like to thank my father Ihsan Mert and mother Nuray Mert for their support to become today's. I would like also to thank to my sister Ayse Yılmaz and her family. I would like to express how much I have loved my mother and father.

ABSTRACT

DIFFERENTIATION OF HEALTHY AND CANCEROUS RENAL CELLS USING SURFACE-ENHANCED RAMAN SCATTERING

Surface-enhanced Raman scattering is used for the differentiation of human kidney adenocarcinoma (ACHN), human kidney carcinoma (A-498) and non-cancerous human kidney embryonic cells (HEK 293). Silver nanoparticles (AgNPs) are used as substrates in the experiments. A volume of colloidal suspension containing AgNPs is added onto the cultured cells on CaF₂ slide and the slide is dried at the overturned position. A number of SERS spectra acquired from the three different cell lines are statistically analyzed to differentiate the cells. Principal component analysis (PCA) combined with linear discriminate analysis (LDA) was performed to differentiate the three kidney cell types with a sensitivity and specificity of 88 % and 84 %, respectively. This study demonstrated that SERS could be used to identify renal cancers by combining this new sampling method and LDA algorithms.

ÖZET

YÜZEYDE ZENGİNLEŞTİRİLMİŞ RAMAN SAÇILMASI KULLANILARAK SAĞLIKLI VE KANSER BÖBREK HÜCRELERİNİN AYIRT EDİLMESİ

Yüzeyde zenginleştirilmiş Raman saçılması (YZRS) insan böbrek kanseri hücre hatları (ACHN, A-498) ile kanser olmayan böbrek hücre hattını (HEK 293) ayırt etmede kullanılmıştır. Gümüş nanoboyuttaki parçacıklar YZRS’de metal katman olarak kullanılmıştır. CaF_2 slaytları üzerinde büyümüş olan hücrelere, kolloid yapıda gümüş nano parçacıkları içeren sıvı karışımdan birkaç damla CaF_2 slaytların üzerine eklenir ve slaytlar ters pozisyonda kurumaya bırakılır. Üç farklı hücre hattından alınan yüzeyde zenginleştirilmiş Raman saçılmaları, model hücreleri ayırt etmek için analiz edilir. Lineer ayırt edebilme analiz (LAA) yöntemi ile kombine esas bileşen analiz (EBA) yöntemi, üç hücre çeşidini sınıflandırmayı 88% hassaslık ile 84 % özgünlükte sağlamıştır. Bu çalışma, yeni örnek hazırlama yöntemi ve LAA algoritmaları ile YZRS’ nın böbrek kanserlerini tanımladığını göstermiştir.

TABLE OF CONTENTS

ACKNOWLEDGEMENTS.....	iii
ABSTRACT.....	iv
ÖZET	iv
TABLE OF CONTENTS.....	vi
LIST OF FIGURES	vi
LIST OF TABLES.....	vii
LIST OF SYMBOLS / ABBREVIATIONS.....	x
1. INTRODUCTION	1
2. THEORETICAL BACKGROUND.....	4
2.1. CELL.....	4
2.2. CANCER	5
2.2.1. KIDNEY CANCER.....	7
2.3. RAMAN SPECTROSCOPY AND RAMAN SCATTERING.....	9
2.4. SURFACE ENHANCED RAMAN SCATTERING.....	11
3. MATERIALS.....	15
3.1. CHEMICALS	15
3.2. CELL LINES	15
4. METHOD	16
4.1. CELL CULTURE METHODS	16
4.2. PREPARATION OF COLLOIDAL SILVER NANOPARTICLES	17
4.3. RAMAN MICROSCOPY SYSTEM.....	18
4.4. PREPARATION OF SAMPLES AND SERS MEASUREMENTS.....	19
4.5. DATA PROCESSING AND MULTIVARIATE ANALYSIS	20
5. RESULTS AND DISCUSSION.....	21
6. CONCLUSION AND RECOMMENDATIONS	30
6.1. CONCLUSION.....	30
6.2. RECOMMENDATIONS	30
7. REFERENCES	32

LIST OF FIGURES

Figure 2.1.	Type of cells: a. plant cell, b. bacteria, c. fungi, d. archaea, e. algae, f. animal cell, and g. Protozoa	5
Figure 2.2.	A schema of kidney cancers: a. kidney cancer stages, b. normal kidney, c. renal cell carcinoma	8
Figure 2.3.	The energy level diagram.....	10
Figure 2.4.	a. Raman spectrum, b. UV/Vis spectra and c. SEM image of AgNPs.....	17
Figure 2.5.	A schematic illustration of the sample preparation.....	19
Figure 2.6.	Image of ACHN cells under 40x objective (a), image of setup used for droplet (b), drying image of droplet area dried at regular position under 4x objective (c), image of droplet area dried at suspended position under 4x objective (d)	21
Figure 2.7.	SEM images of ACHN cells before (a) and after (b) treatment with AgNPs containing colloidal suspension.....	22
Figure 2.8.	Mean SERS spectra from cultured cells; ACHN, A-498 and HEK 293. (a) Mean SERS spectra from HEK 293, a-498 and ACHN cultured cells. Spectra have been normalized to the intensity 529 cm^{-1} peak (b).....	24
Figure 2.9.	2D Euclidean distances plot constructed from the arbitrarily chosen 33 spectra obtained from each cell lines (a), and 2D Euclidean distances plot of the one averaged spectra from 3000 SERS spectra for each cell line (b)..	27

Figure 3.1. The PC scatter plots show the principal components of 30 cells from each cell lines (ACHN, A-498, and HEK 293). PC 1 and PC 2 (a), PC 1 and PC 3 (b), PC 2 and PC 3 (c), PC 1 and PC 4 (d), PC 2 and PC 4 (e), PC 3 and PC 4 (f)..... 28

Figure 3.2. LD 1 and LD 2 scatter plot of three types of cells..... 29



LIST OF TABLES

Table 4.1. The band assignments of SERS spectra of the cell lines	26
---	----



LIST OF SYMBOLS / ABBREVIATIONS

AgNPs	Silver nanoparticles
DLS	Dynamic light scattering
DNA	Deoxyribonucleic acid
FTIR	Fourier transformed infrared spectroscopy
RCC	Renal cell carcinoma
Wt1	Wilms tumor protein
IR	Infrared
Mg	Milligram
mW	Miliwatt
MW	Molecular weight
Nm	Nanometer
PBS	Phosphate Buffered Saline
SEM	Scanning electron microscopy
SERS	Surface-enhanced Raman scattering
UV/Vis	Ultraviolet/Visible
ATCC	American Type Culture Collection
ATP	Adenosine triphosphate
DMEM	Dulbecco's Modified Eagle Medium
DMSO	Dimethylsulfoxide
M	Molar
ml	Milliliter
ng	Nanogram
s	Second
h	Hour

1. INTRODUCTION

Cancer continues to be one of the deadliest diseases worldwide. In last two decades, a significant effort has been devoted for the diagnosis and treatment. However, the diversity of the causes resulting in malignancy hinders the development of a solid approach for treatment. Therefore, early diagnosis gains importance for successful treatment of the disease. Conventional cancer diagnostic approaches such as Positron Emission Tomography (PET), Computed Tomography (CT), Magnetic resonance (MR), and ultrasound are routinely used for the cancer diagnosis [1]. MRI identify changes in the tissue morphology due to abnormal cell growth while PET gives information about malignant tumors where cellular activity is increased [2]. These techniques provide information about the disease development mostly after early stage of the cancer development.

The use of spectroscopic approaches such as fluorescence [3], infrared [4] and Raman [5] spectroscopic techniques are gaining importance in clinical research in recent years since they can provide fast molecular level information with minimal surgical intervention or biopsy [6]. The utility of vibrational spectroscopic techniques, IR and Raman, has long been investigated for tissue differentiation [7-9]. A Raman spectrum can give direct information about molecular composition of a sample. This non-destructive and non-invasive technique was employed for population investigation for early diagnosis and following phases of treatments [10]. Especially Raman spectroscopy was used to examine tissue samples obtained from breast [11], brain [7], cervical [12], nasopharyngeal [13], lung [14] and skin [15].

Surface-Enhanced Raman Spectroscopy (SERS), can be considered as a mode of Raman Spectroscopy, and allows the enhancement of Raman scattering up to 10^8 when molecule or molecular structure is located in the close vicinity of nanostructured noble metal surface [16]. The sensitivity increase in SERS resulted in an enormous interest from the scientific communities from various disciplines to employ the technique for detection and identification of DNA [17], proteins [18], microorganisms [19] and living cells [20] and tissue [7].

The first use of SERS at the living single cell level for the detection of low-level antitumor drug concentrations was reported in 1991 [21]. Shortly after, a pioneering study was demonstrated that SERS could be used to collect biomolecular information from living cells at single cell level [20]. In that study, gold nanoparticles (AuNPs) internalized by the cells were used as substrates. In the following years, several reports concerning the use of SERS of living cells were appeared in the literature [14,22-31]. All these studies demonstrate that SERS is slowly evolving as a novel technique to obtain molecular level information at single cell level.

Kidney cancer is almost 2% of all cancer cases around the world [32]. Although the most common form of kidney cancer, renal cell carcinoma (RCC), has increased in the west compared to Asia [33]. The RCC has similar symptoms with many diseases. Only about 5% to 10% people with RCC shows classic symptoms such as abdominal mass, flank pain, and hematuria, and only 9% of RCC cases appear with the symptoms abdominal mass, flank pain, and hematuria [34]. Therefore, the symptoms of RCC can be easily confused with other diseases, and it makes diagnosis very difficult. With early diagnosis, the RCC patients have high survival rate. The research over past thirty years on early detection, diagnosis and treatment for patients with RCC has been increased and provided new imaging techniques for the tumorous formations [35].

In this study, the multidimensional scaling method was used to differentiate the healthy and cancer cells. The multidimensional scaling method based on the similarities and dissimilarities between the data. A MDS algorithm begins with a matrix of the objects according to similarities. The objects are placed on the plot with the distances, which display the dissimilarities between them. MDS method uses new variables, reduced from original variables. The plot is placed in multidimensional space according to the number of variables. The distance of variables on the plot is measured as Euclidean distance [36].

In our study, we demonstrate the power of SERS using citrate reduced AgNPs as substrates for the differentiation of cancer and healthy kidney cells. ACHN cells with higher tumorigenic and metastatic potentiality, A-498 cells with lower tumorigenic potentiality and HEK 293 (non-cancerous) cell were chosen as model cells. The sample preparation method that we employed in our previous study for protein detection and identification

with SERS was used in the study [37]. The method uses the drying of sample containing colloidal AgNPs and analyte at the overturned position. This allows more uniform distribution of AgNPs on the droplet area instead of getting them jammed at the liquid-air-solid contact interface. The SERS spectra obtained from three cell lines were processed with LDA based on PCA method to differentiate the healthy cells from cancer cells. The results of this study with a sensitivity of 87, 8% and specificity of 84, 4 % indicate that the SERS spectra obtained from the cells can be used for cancer diagnosis.



2. THEORETICAL BACKGROUND

2.1. CELL

The word cell has the meaning of “small room”, which originates from Latin word *cella*. The cell is the main biological and functional unit of living organisms. They are called as building block of life and they are the smallest living unit except viruses, which have only DNA or RNA. The number of the cell in plants and animals vary species to species. A healthy human has about 100 trillion cells. The cells are visible only under a microscope. The cell was first determined by Robert Hooke in 1665. The cell theory was developed by Matthias Jakob Schleiden and Theodor Schwann in 1839. Organisms are formed by one or more cell according to the theory. The cells have hereditary information, which provides cell regulation functionality and transfer these data to the next generation by cell division.

The main components of cell in both animal and plants are plasma membrane/ cell membrane, cytoplasm and nucleus. The cell membrane has a bilipid layer containing proteins and carbohydrates in its structure. It protects the cell from outer affects and gives stability to the cell. Therefore, the plasma membrane provides the transportation of materials. The cytoplasm of the cell contains organelles, which have vital roles for function and regulation. The nucleus, largest organelle, covered by double nuclear membrane is the control center of the cell for cell metabolism and reproduction. It has the genetic information called as DNA on chromosomes.

Protists, fungi, plant and animal cell are eukaryotic cells while bacteria and archaea are prokaryotic cells (Figure 2.1). There are two primary types of cells, which are prokaryotic and eukaryotic. They have much dissimilarity between them such as organelles, size, cell division etc.

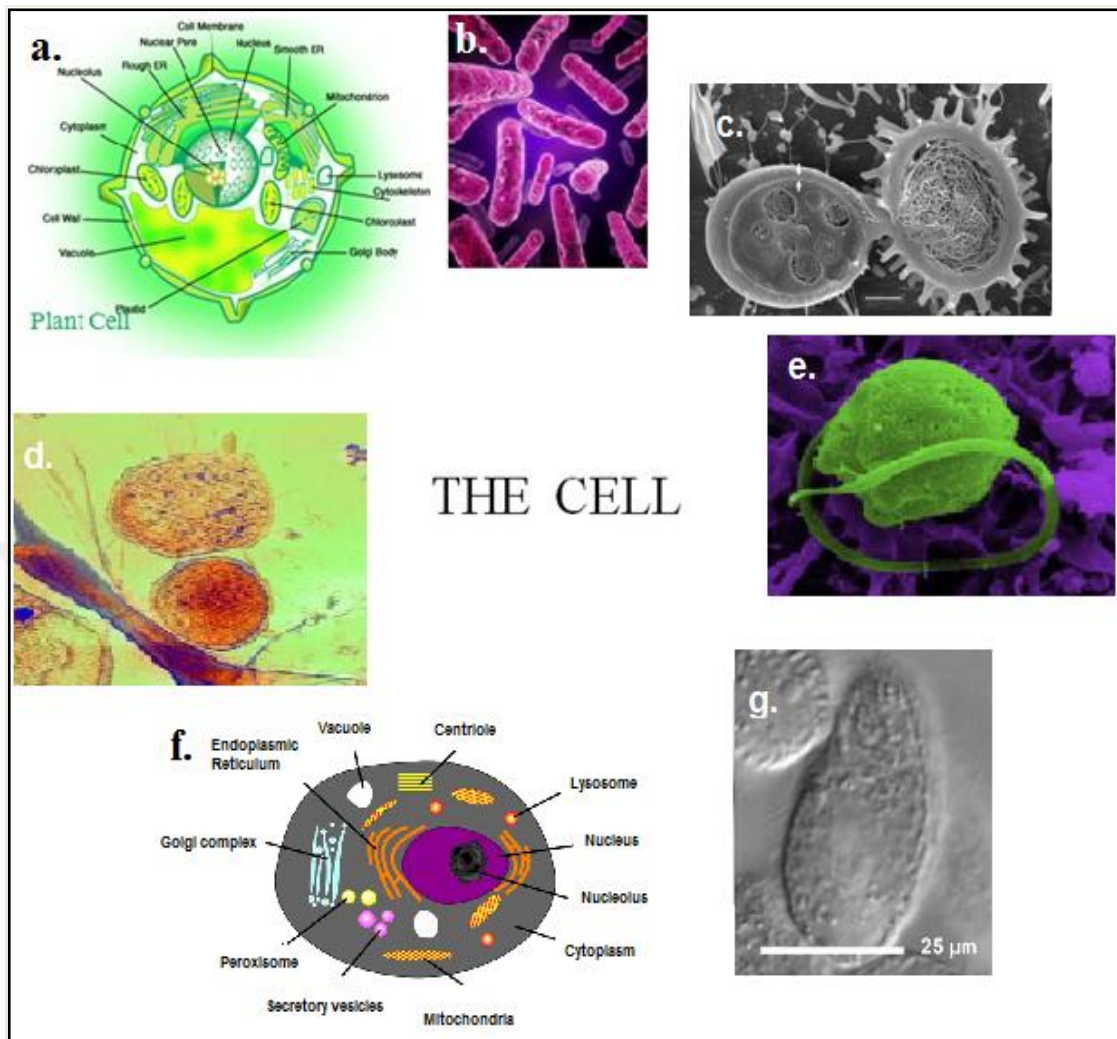


Figure 2.1. Type of cells: a. plant cell [38], b. bacteria [39], c. fungi [40], d. archaea [41], e. algae [42], f. animal cell [43], and g. protozoa [44]

2.2. CANCER

The term “tumor” was initially applied to the growth caused by inflammation. Oncology (Greek “oncos”= tumor) is the search of tumors or neoplasms, a new abnormal growth of the tissue. Cancer is the general name for all malignant tumors.

Cancer is a complex genetic disease, and some environmental factor caused the cancer disease. For example, the cancer-causing agents (carcinogens) can be found in anywhere such as food, water, air. The sunlight exposure can also be another example for the cause of the cancer. There were approximately 10 million new cancer cases in 1996 all over the

world and six million of deaths attributed to the cancer [45]. It is for seen that there will be 20 million new cases and 12 million deaths due to cancer by 2020 [46]. Ageing of population and the globalization of unhealthy lifestyles with smoking and fast foods with high fat, and low fibre content might be causes contributing to cancer incidences [47].

There are two types of tumors, benign and malignant. Each benign tumor which has slower growing rates than malignant tumors has an ability to invade surrounding tissue or metastasis, final state of the cancer diseases. Even though, benign tumors are very similar to their tissue of origin, malignant tumors are dissimilar to their origin tissue. Benign tumors are grown properly by pushing the environmental textures, and they have boundaries with tissue so that they can be separated from the tissue easily with surgical intervention. However, malignant tumors are grown in an unregulated way by invading and destroying the healthy tissue by moving around with a colonized cancer cells, and they can circulate to other body organs. The surgical intervention is difficult due to invasion. The potential of recurrence after surgical removal is rarer in benign tumors than malignant tumors. Necroses in malignant tumors are more common rather than benign tumors. If the benign tumor is not a secreting endocrine neoplasm, they don't have life threaten effects for the body.

Since it may develop into malignant phase, the benign tumors should be removed. The malignant tumors not only surround the tissue, but also are able to colonize. The malignant tumors fall into two groups, sarcoma or carcinoma. Sarcoma is the malignant tumor grown in connective or muscle tissue and uses the blood stream to spread. The carcinoma is most common type of the malignant tumor, which grows in epithelium, and uses the lymphatic system to spread through the body. The malignant tumors cause the metastasis and the patient death when they are at the latest stage. The colonized metastatic cancer cells spread to the vital organs and degrade the organs rapidly. The early detection is the most important to treat patients with cancer. The richer and developed countries have some programmers such as cervical screening, mammography, colonoscopy or occupation to monitor the possible future cancer patients [48]. These programs provide early detection of the cancer.

The remove of the tumors by surgery is the most effective way for treatment of the cancer. The targeted radiotherapy, which is a combination of anticancer drugs, is another option for treatment. Most of the anticancer drugs were designed to interfere with DNA synthesis. The anticancer drugs also cause damage in healthy cells such as bone marrow cells, which generate red blood cells and cells to fight infections [49]. Therefore, patients receiving chemotherapy face unwanted side effects such as anemia and hair loss [50]. Another method is focused on attempting to target tumor cells. They are combined the cell toxins to tumor specific antibodies to slow down the cancer progression by impacting cell adhesion, proteolytic enzyme activity and angiogenesis [51].

2.2.1. KIDNEY CANCER

Kidney cancer is classified into two types. The renal cell carcinoma (RCC), which initiates from the renal parenchyma and the renal transitional cell carcinoma (RTCC), which comes from the renal pelvis. In children, mostly the nephroblastoma also known as Wilms tumors are resulted from a mutation in transcription factor Wilms tumor protein (Wt1) [52]. It was demonstrated that RCC generates approximately 90% of kidney cancer and RTCC is less than 10% of kidney cancer [33].

Cancer statistics states that kidney cancer comprises just about 2% of all cancer types in the world with 200,000 new cases and 100,000 deaths per year [53]. The rates of kidney cancer in men and women are 2.5% and 1.7% [54].

Renal cell carcinoma (RCC) is the common type of kidney carcinoma that embraced 90% of kidney cancer cases [55]. The death ratio of RCC is higher than other urological cancers and RCC is more resistant to radiotherapy and chemotherapy treatments [56].

Grading is one of the analytical features in the management of RCC. Related to other cancer types, TNM (Tumor, Node, and Metastasis) arrangement is generally used in RCC [57]. The grading system demonstrating the anatomical extension of tumor, dispersion to regional lymph nodes and distant metastasis is mainly used in RCC as predictive factor.

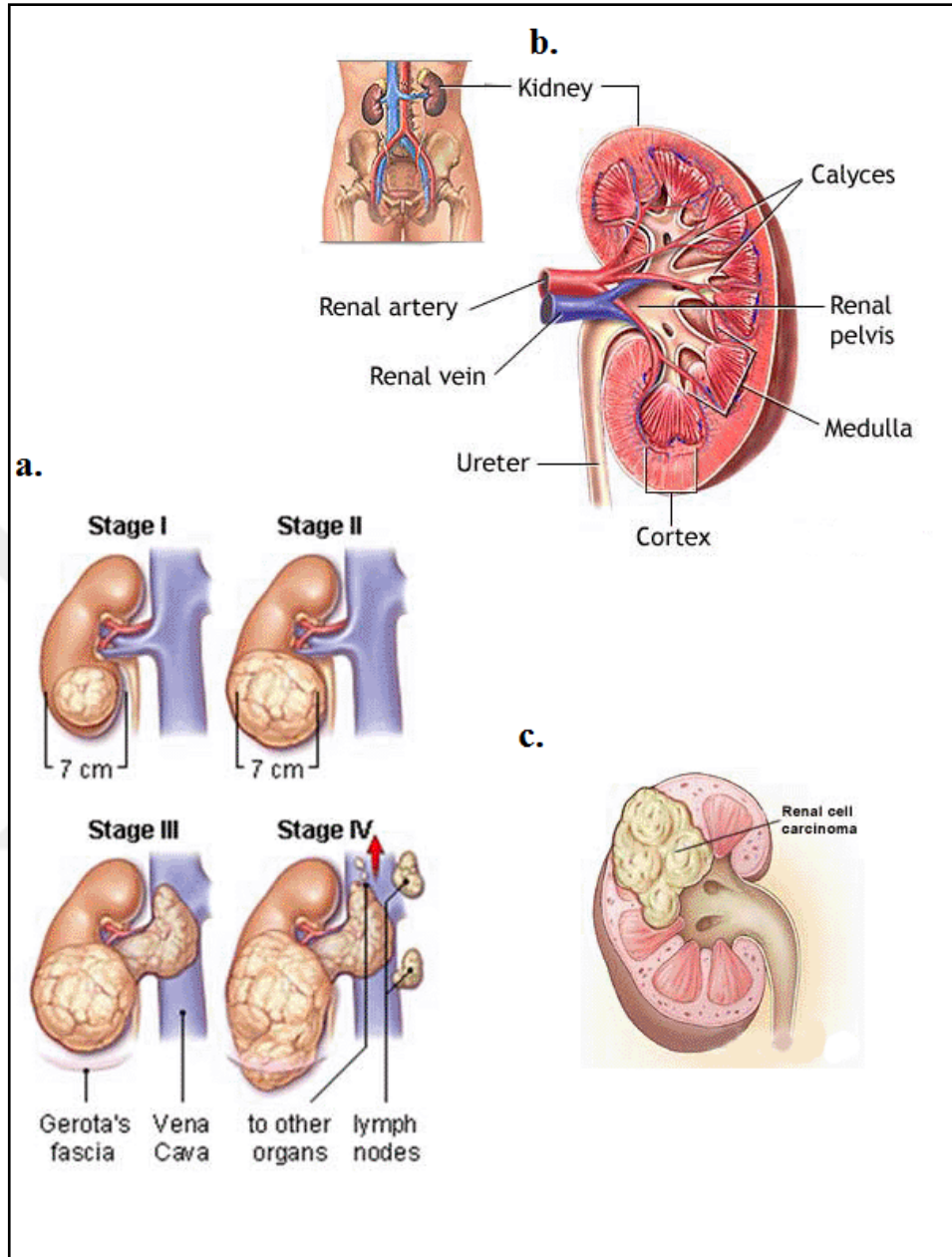


Figure 2.2. A schema of kidney cancers: a. kidney cancer stages, b. normal kidney, c. renal cell carcinoma [58]

2.3. RAMAN SPECTROSCOPY AND RAMAN SCATTERING

Raman was firstly observed by Dr. Chandrasekhar Vanuatu Raman in 1928 [59]. It took a long time for the development of modern Raman spectrometers. This is mostly due to the development in laser and detector technology since Raman scattering is inherently very weak. It has become an important analytical tool in biophysics, biochemistry and biomedicine in recent years. Today's Raman instruments are highly specialized for the use by researcher. Raman is now used in very areas such as chemistry, biology, geology, pharmacology, medicine, materials science and pharmaceuticals because of having high sensitivity, meaningful information and non-destructive properties. Raman spectroscopy provides direct identification of analyst of interest.

After a sample is irradiated with a powerful monochromatic light source, which is generally a laser, most of the radiation is scattered by the sample induced at the same wavelength [5]. The case of the incident and the reflection of the radiation in same wavelength called as Rayleigh scattering [60].

The molecule in the ground vibrational and electronic states is shown in the energy level diagram (Figure 2.3). The energy of the mechanism is increased by the electric field of the laser beam immediately while inducing a polarization in the molecule. Relaxation is the transition of the molecule from a higher level to a lower one. Relaxation outcomes in Rayleigh scatter. When the relaxation is occurred to the first stimulated vibrational state, the scattered light will be at lower energy (longer wavelength) than the laser wavelength. This process called as Stokes-Raman scattering. When the Raman process is triggered from the excited vibrational states, the relaxation would be to the ground state. This is called anti-Stokes Raman scattering. Since this vibrational state which is less energetic than the initial state.

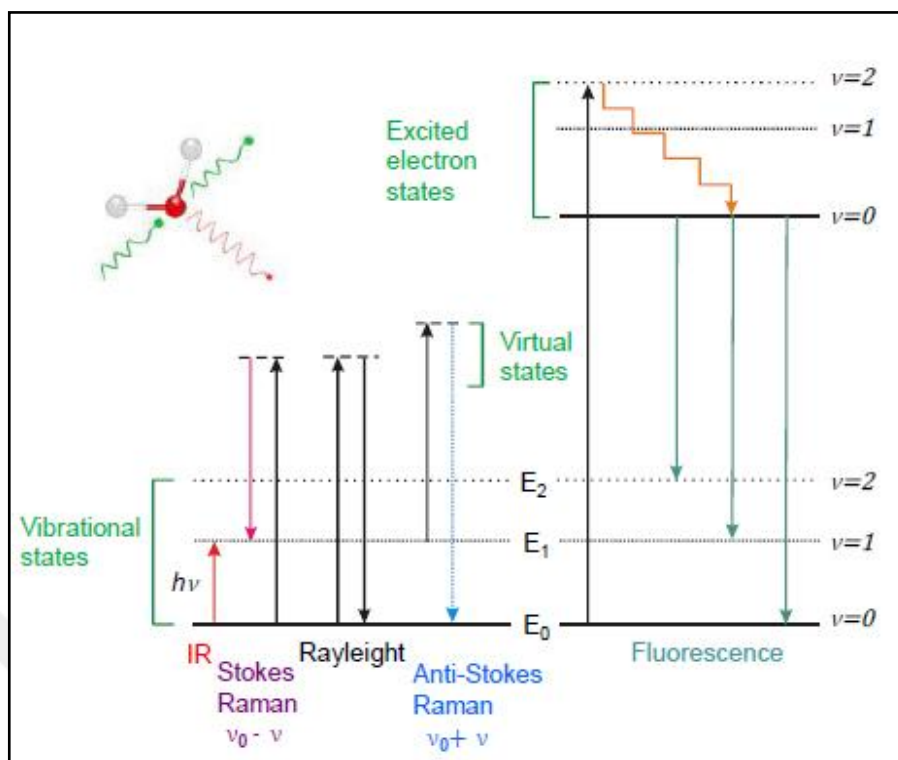


Figure 2.3. The energy level diagram [60]

In most cases, fluorescence spectral bands are broader than Raman spectral bands [61]. The fluorescence spectra do not provide much information about the structure of a molecule. Thus, Raman spectra give more information about the atoms, bond strengths and organization in a molecule. In addition, Raman spectra obtains a fingerprint for the structure of the molecule [62]. Raman spectroscopy holds very significant information about the structure of molecules. The position and intensity of features in the spectrum displays the molecular structure and can be helpful in the determination process of the chemical identity of the sample. Depending on the crystalline form, spectra might also show small changes.

When compared with other analytical techniques, Raman spectroscopy has more advantages. Raman is a scattering technique, thus placing the sample under the excitation beam and collecting the scattered light is all that is needed for the collection of a spectrum [5]. Raman is more sensitive to symmetric bonds and backbone structures. Raman spectroscopy has more advantages such as minimum sample preparation step,

spectral acquisition directly from sample, minimal water intervention and no intervention from atmospheric CO₂.

2.4. SURFACE ENHANCED RAMAN SCATTERING

Surface-enhanced Raman scattering (SERS) is the phenomenon that gives rise to the enhancement of Raman scattering up to 10^8 on nanostructured noble metal surfaces. Although the enhancement of Raman scattering of pyridine on a silver electrode was reported in 1974 and explained with the increased concentration effect on the electrode surface [63], its mechanism was explained by two different mechanisms, electromagnetic and chemical by Jeanmaire and Van Duyne and Albrecht and Creighton, respectively, in 1977 [64,65].

The intensity of Raman signal of adsorbents on particle surfaces is increased because of the enhancement in the electric field produced by the surface and charge transfer between adsorbed molecule and the noble metal surface. The first process is related to electromagnetic field enhancement. After the incident light contacted with the surface, surface plasmons will be excited. The scattering happens when the plasmon oscillations are perpendicular to the surface [66]. As a result, the roughened surfaces and arrangements of nanoparticles are engineered for the SERS experiments to obtain a localized collective oscillation to enhance the Raman signals [67-69].

The choice of the metal surface depends on the plasmon resonance frequency of metal. In order to obtain optimally enhanced scattering in visible and NIR of spectrum, the silver and gold nanosized materials are used as SERS substrates [70]. The other metals such as copper, platinum and palladium can support for the formation of surface plasmons but they are not preferred due to their high reactivity and impractical experimental conditions for surface plasmon excitation [71-73].

A molecule adsorbed to the surface with a free pair of electrons have been also displayed a different enhancement mechanisms, which is different from electromagnetic enhancement related to surface plasmons. This mechanism is the result of chemical absorption of the molecule onto the metal surface causing a charge transfer between the metal and the molecule [74].

There are several configurations constructed from silver and gold using variety of techniques including lithography reported in literature [75-78]. Although, a certain degree of success could be achieved with prepared substrates, the results vary depending on the application type. The substrates can be classified into groups depending on the way they constructed, surfaces and colloidal nanoparticles. Although, both types of substrates are widely used, the latter found wide spread use due to their simple and cost effective preparation. With the fact that the highest enhancement was reported on AgNPs clusters, the AgNPs are now routinely used as SERS substrates.

The colloidal AgNPs and AuNPs can be synthesized by using many different reducing reagents or by laser ablation as solid silver or gold [79-83]. In many studies, citrate-reduced NPs are used as SERS substrates because of high SERS effect and stability.

The effort to use of SERS in the biophysical, biochemical and biomedical fields has dramatically increased after early 1990s [84-88]. The several reports are available about the SERS of amino acids, peptides, and DNA, RNA and nucleotide bases in literature [62,89-97]. Therefore, the SERS studies were also performed on colored biomolecules such as chlorophylls and the other pigments [98]. Also larger molecules, proteins, containing chromophores such as heme group were studied with SERS. The SERS studies in medical field are mostly applied to detection of stimulating drugs and antitumor drug interaction with DNA [21,99]. The SERS technique is not only interested for ultrasensitive detection and characterization of biomolecules but also used in biophysical process. For instance, it was used to demonstrate the transportation through membrane [100]. It was shown that the SERS can differentiate the movement of unsimilar molecules across a membrane and also observed the arrival time of the transporter molecule and concentration growth rate in colloidal AgNP suspensions. SERS was also utilized for studying charge transfer mechanisms; for example in cytochrome c, which has been explored on bare and coated silver electrodes [101].

The rapid detection of microorganisms is significant because of the increase of infections rates. SERS is a valuable technique due to the minimal sample preparation to identify bacteria based using their SERS spectrum. One of the early SERS studies of microorganism had used colloidal silver nanoparticles as SERS substrate [98]. The AgNPs

are produced with microorganism and its wall by forming a rough silver coating. The SERS signals have been used the characterization of the bacterium due to the enhancement factors. Although the SERS spectra were collected 1-2 mW laser excitation in a few seconds, bulk Raman spectrum of bacteria show weak even with the use of 100 mW laser power with 30-60 min collection time [102].

SERS was also used for the characterization of living cells [21,103]. The first use of SERS at the living single cell level for the detection of antitumor drug concentrations was reported in 1991 [21]. In another study, the SERS spectra has been measured by incubating intestinal epithelial cells (HT29) with colloidal AuNPs [20]. A recent study about the release of anticancer drug combinations from AuNPs in K562 human myeloid leukemia cells was performed [104]. They generated an anticancer drug as a BCR-ABL tyrosine kinase inhibitor on AuNPs surfaces along with a transferring (Tf)-targeting component to treat the leukemia cells. In another study, SERS is used to investigate cellular surface of immunolabeled endothelial cells [105]. Immunolabeling process was carried on in two steps. The first step was coupling of gold-conjugated antibodies. In the second step, the attachment of the AgNPs to cell surface was performed. The bands on the SERS spectra originating from cell membrane components were observed. The direct relationship of the membrane components with the distribution of AgNPs provides a spectral mapping by SERS also used in that study. Another interesting study was about the detection of single apoptotic cells [106]. AgNPs-decorated silicon wafer (AgNPs@Si), as a high-performance in vitro sensing platform for the detection of single apoptotic cells was employed. In another study, nanoparticles are used for targeting tumors in vivo [14]. The colloidal AuNPs were pegylated and used in vivo tumor targeting. The several SERS studies on the cell are available in the literature [14,22-31,107-113].

In almost the entire SERS- living cell studies reported in the literature, the AuNPs were used as substrates after up taken by cells and relate the spectral changes to the metabolic activity of the cell. In this thesis, an unusual approach for the sample preparation was employed as different from the ones reported in the literature. The AgNPs and/or the aggregates are distributed onto the cells grown on a slide. The aim was to bring the biomolecular structures and AgNPs from as many as different points on the cell surface. The cells placed onto the CaF₂ were dried and a small volume of AgNP colloidal

suspension was placed onto the cells and dried at the overturned position that brings the colloidal droplets to the suspended position. This configuration prevents the “coffee-ring” formation phenomenon, which causes the jamming of all AgNPs at the droplet peripheral. Our group in previous studies demonstrated the usefulness of the suspended droplet approach for the detection of proteins.



3. MATERIALS

3.1. CHEMICALS

Sodium citrate (99%) was purchased from Merck. AgNO_3 (99, 5 per cent) was purchased from Fluka. PBS was purchased from Hyclone. Dulbecco's Modified Eagle's Medium – high glucose and Fetal Bovine Serum (FBS) was purchased from Sigma. L-Glutamine was purchased from Invitrogen. Penicillin-streptomycin was purchased from Thermo Scientific. Trypsin-EDTA was purchased from Biochrom.

3.2. CELL LINES

RCC cell lines, HEK 293, A-498 and ACHN were purchased from ATCC.

4. METHOD

4.1. CELL CULTURE METHODS

Renal cancer cells (ACHN and A-498) and normal cells (HEK 293) were obtained from American Type Culture Collection (ATCC). ACHN cell line has high tumorigenic properties, while A-498 cell line has low tumorigenic properties. Thus, HEK 293293 is non-cancerous and immortalized cell line. The cells were taken out from 80°C freezing icebox, thawed, and washed. Then, ACHN, A-498 and HEK 293 cells were incubated in T-75 flasks using glucose Dulbecco's modified Eagle's medium (DMEM) (Sigma-Aldrich, Germany) with the 10% fetal bovine serum (FBS), 2 mM L-glutamine and the 1% penicillin/streptomycin in an incubator humidified 5% CO₂ atmosphere at 37°C prior to subculturing. For subculturing of HEK 293-293 cells, the medium was removed and rinsed with phosphate buffered saline (PBS, 10X) solution, and a 2 ml of 0.025% trypsin solution was added into the culture plate and placed at 37°C until the cells detached. Then, the fresh medium was added to deactivate trypsin, and the cultures were transferred into the centrifuge tubes and centrifuged at 1500 rpm for 5 min. After the supernatant was removed, the fresh medium was added and dispensed into a new flask containing the fresh medium. For subculturing of ACHN and A-498 cells, the medium was removed and rinsed over the adherent cells using PBS. Then, a 2 mL of 0.025% trypsin was added and the culture was incubated at 37°C for 10 minutes. The culture were transferred to centrifuge tubes and centrifuged at 1500 rpm for 5 min. After the supernatant was removed, the fresh medium was added and dispensed into new flasks containing fresh medium. After the twice subculturing, the cells were moved to 6-well cultivation plates with CaF₂ slides and incubated at 37°C. The cells were directly grown on CaF₂ slides using standard procedure. Before the SERS measurements, the culture medium was removed and the cells were washed three times with PBS. Then, CaF₂ slides were rinsed with water to remove remanant salts. After the CaF₂slides were dried, a 2-μL of colloidal AgNPs was added onto the slides, and the slides were turned upside down to dry in cell culture hood in sterile conditions.

4.2. PREPARATION OF COLLOIDAL SILVER NANOPARTICLES

The colloidal AgNPs were synthesized by using sodium citrate as reducing agent [70]. Briefly, a 90 mg of AgNO_3 was dissolved in 500 mL of water, and the solution was kept on the heater until boiling. Then, a 10 mL of 1% sodium citrate was added into the solution and the solution was kept one and half hour until the volume reached the half volume. The concentration of this suspension was called 1X. The final concentration of AgNPs colloidal suspension was adjusted to 4X by centrifuging the 1X suspension and removing the $\frac{3}{4}$ of the supernatant for the use in SERS experiments. The average size distribution of the solution was around 60 nm and the maximum absorption was recorded at 420 nm. The characterization was performed by UV/vis Spectroscopy (Perkin Elmer Lambda 25-UV), Zetasizer NanoZS (Malvern, UK), SEM (Carl Zeiss Evo 40) and Raman spectroscopy (Figure 2.4). The colloidal silver solution had an absorbance at 420 nm and the size distribution was averaged as around 60 nm.

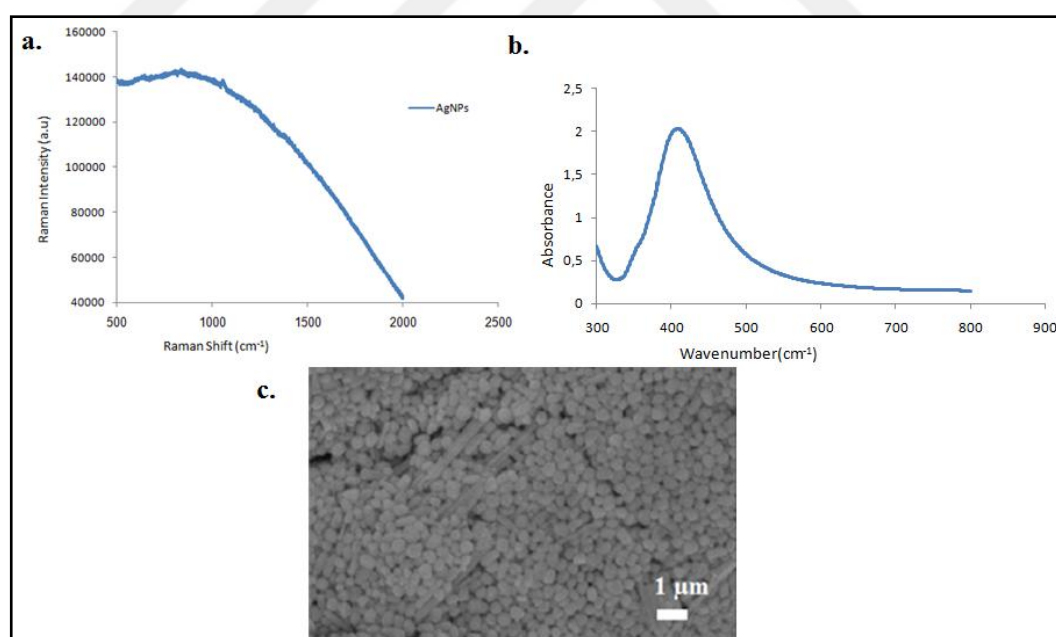


Figure 2.4. a. Raman spectrum, b. UV/Vis spectra and c. SEM image of AgNPs

4.3. RAMAN MICROSCOPY SYSTEM

A Renishaw InVia Reflex Raman microscopy system (Renishaw Plc., New Mills, and Wotton-under-Edge, UK) equipped with an 830 nm diode was calibrated by using the silicon phonon mode at 520 cm^{-1} . The incident laser power was 7.5 mW on the sample and the spectral data acquisition time was 10 s. A 50× microscope objectives (NA: 0.50) was used in the experiments. The SERS spectra were acquired over a spectral range of 500-1800 cm^{-1} because the specific Raman bands were observed in this range. The SERS spectra were collected over an area of $10 \times 10\ \mu\text{m}^2$ on the cell in 1- μm steps by using map image acquisition method. The experiment was repeated at least three times, and the spectral analyses were carried out by the WIRE 2.0 software.

4.4. PREPARATION OF SAMPLES AND SERS MEASUREMENTS

After the cells were grown on CaF_2 slides, the culture medium was removed and the cells were washed three times with PBS. Then, CaF_2 slides were rinsed with water to remove remenant salts. After the CaF_2 slides were dried, a 2- μL of colloidal AgNPs was placed onto the slides, and the slides were turned upside down to dry in cell culture hood in a sterile condition.

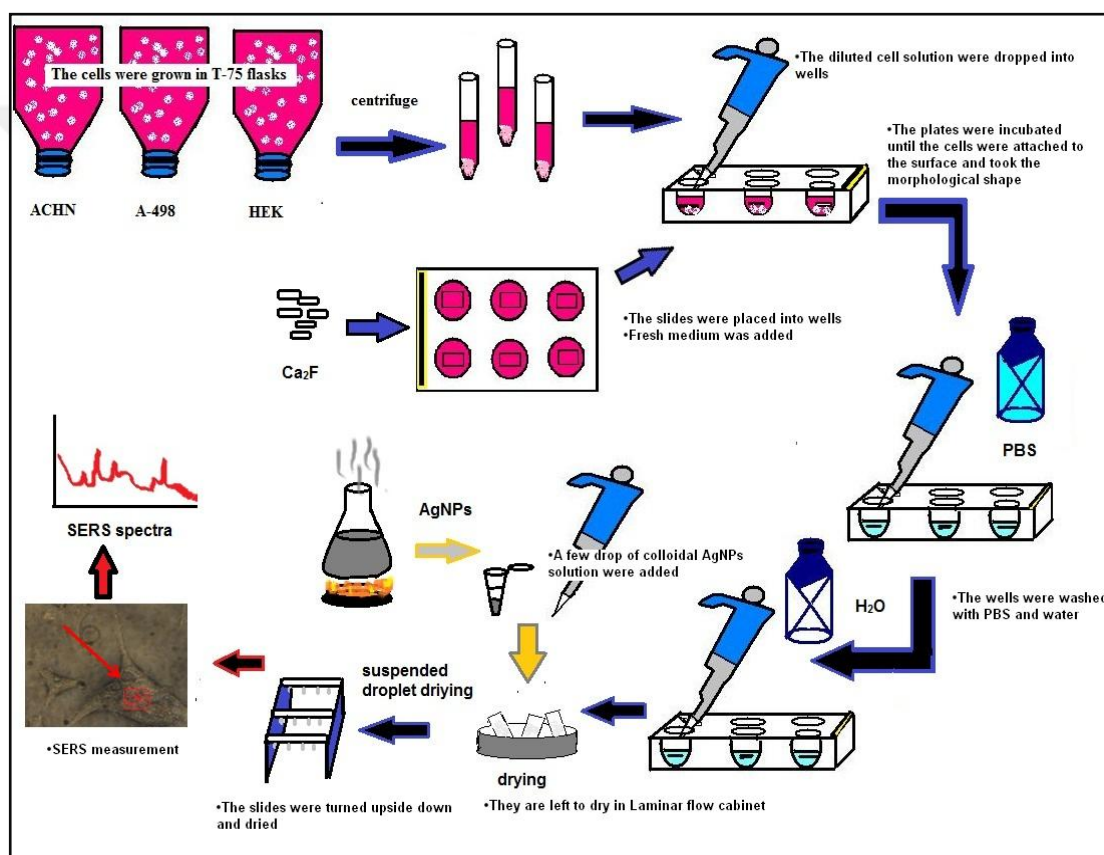


Figure 2.5. A schematic illustration of the sample preparation

The experiment was repeated at least three times. Each step of the experiment involves SERS mapping of the cell in $10 \times 10 \mu\text{m}^2$ areas with 1- μm steps. As a result, one hundred SERS spectra from a minimum 30 selected cells from each cell lines were acquired. Each of cell lines has a minimum of 3000 SERS spectra collected.

4.5. DATA PROCESSING AND MULTIVARIATE ANALYSIS

The total number of spectra collected on a cell over $10 \times 10 \mu\text{m}^2$ area was 100. A minimum of 30 cells for each cell lines was used for the SERS acquisition for each experiment. Each of 100 SERS spectra obtained from each single cell was normalized to reduce the variations in intensity, and the total SERS spectra obtained from each cell were averaged to obtain a mean SERS spectrum. The SPSS software package (SPSS Inc., Chicago) was used for multidimensional scaling method (MDS) [36] by performing the Euclidean distance method, which was introduced on the SERS spectra to see the similarity and dissimilarity of the collected cell spectra. Then, the linear discriminant analyses (LDA) [114] method was used as classification method. Principal component analyses (PCA) [115] was used to reduce the dimension of the SERS spectral data set space by generating standardized matrices, and to produce PC scores, which are the most significant variables produced from original spectra. PC scores were used as variables in LDA method. The LDA provides discriminant functions, which increase the variances in SERS data between different cell lines while decrease the variances between the cells of the same cell line.

5. RESULTS AND DISCUSSION

The CaF_2 slides were used to culture the cells due to the interference from the glass background during the spectra acquisition from the cells placed on glass slides. After they were grown, the medium was removed by washing with PBS, and PBS was washed by filtered and autoclaved water to avoid contamination. Therefore, they were placed in cell culture hood until drying. Then, a 2- μl droplet of colloidal suspension containing AgNPs were added onto the cells under light microscope and left to dry by turning upside down. Multiple 2 μl droplets were spotted onto the cells grown on CaF_2 slide in order to place the AgNPs on more cells when necessary. A 40 \times microscope objective was used to observe the location of the cells, and the aggregation of AgNPs in dried droplets for each position, under 4 \times objective (NA: 0.13) is visual in Figure 2.6.

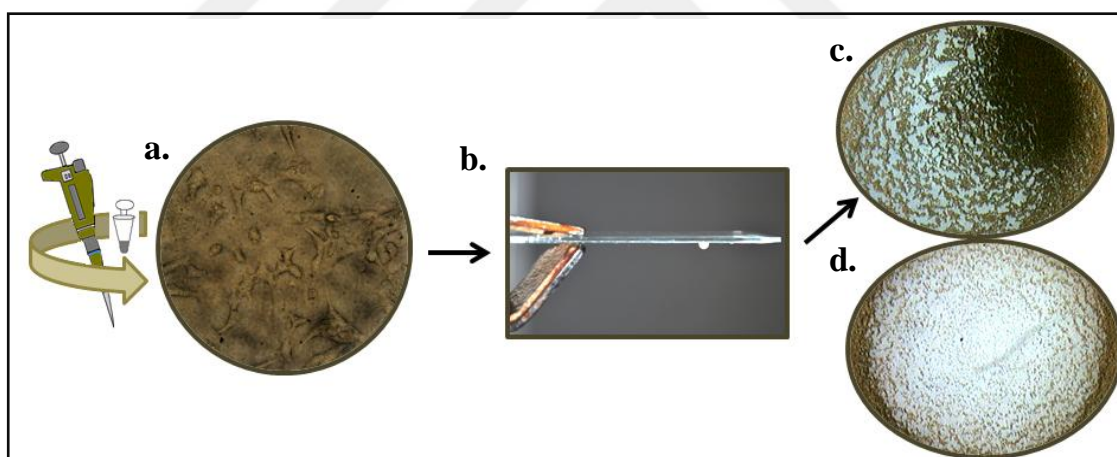


Figure 2.6. Image of ACHN cells under 40x objective (a), image of setup used for droplet (b), drying image of droplet area dried at regular position under 4x objective (c), image of droplet area dried at suspended position under 4 x objectives (d)

When a small volume of colloidal suspension containing AgNPs is placed on a surface, a phenomenon called “coffee-ring” takes place and jams almost all of the particles at the liquid-solid-air interface. This causes the formation of very tightly packed particles at the droplet edges [116,117]. For optimal SERS activity, a loose packing of noble metal particles is necessary. [118-120]. In order to avoid the unequal distribution of AgNPs on the

droplet area and jamming them at the droplet peripherals, the droplet placed onto the cell grown on CaF_2 was overturned and dried at the suspended position (Figure 1 b). Figure 1 c and d show the comparison of the droplet areas at the suspended (c) and regular position (d). As seen, the clusters of AgNPs are mostly observed at the center of the droplet when droplet is dried at regular position while they are fairly distributed in the droplet area dried at the suspended position.

The cells grown on CaF_2 are washed with PBS and then water before they let drying at room temperature. During drying, it highly possible that the most of the cells retained their morphology while a few of them crystallized. Washing procedure of the cells grown on CaF_2 makes the cells, with retained morphology (see Figure 1 a) visible to select them under microscope during the addition AgNPs colloidal suspension on it, and the selection of them for SERS measurement. Since the cells are intact and dried, the addition of the AgNPs colloidal suspension does not alter the cell morphology. The SEM images of ACHN cells before (a) and after (b) addition of the AgNPs colloidal suspension are given in Figure 2.7. As seen, the addition of colloidal suspension damages the cell integrity. Cell necrosis, unprogrammed death may be resulted because of unexpected condition, drying and adding colloidal suspension during the sample preparation. However, the AgNPs and their aggregates are remained in the ruptured cell area. Therefore, the spectral features on the SERS spectra may originate from biomacromolecules and ionic species composing the cell.

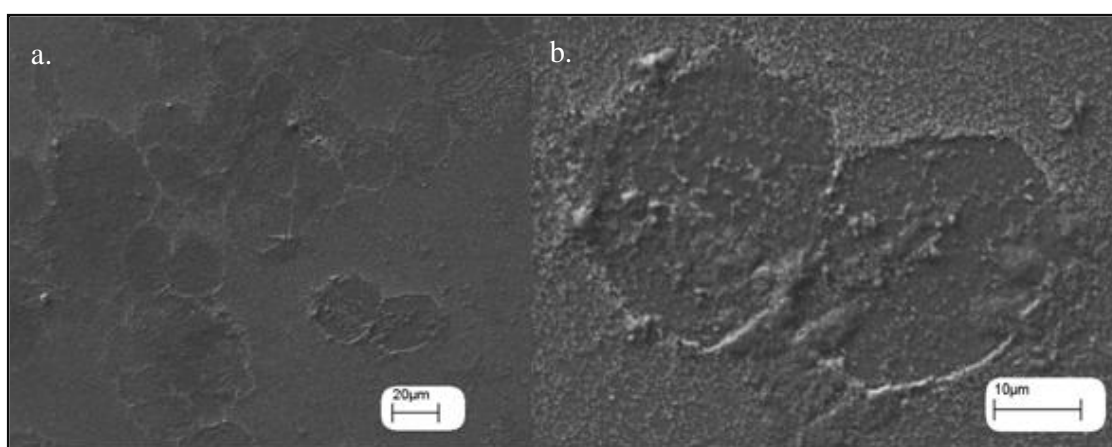


Figure 2.7. SEM images of ACHN cells before (a) and after (b) treatment with AgNPs containing colloidal suspension.

The approach of SERS measurement were employed from an area of $10 \times 10 \mu\text{m}^2$ onto cell by using map image acquisition method with $1 \mu\text{m}$ steps. A total of 100 SERS spectra from one cell (a minimum of 30 cells for each cell line) were acquired with an 830 nm diode and a 50 x objective. The laser power of the incident light was 7.5 mW, which couldn't damage the cells, and the best SERS spectra were obtained in this value of the power. Almost 3000 SERS spectra for each cell line were collected, and the total SERS spectra acquired from healthy and cancer cell lines were averaged to one mean SERS spectra are presented in Figure 2.8 (a), and the mean SERS spectra for each cell line was normalized at 529 cm^{-1} (b). The normalization of the spectra at 529 cm^{-1} was processed supposing the Raman intensity for each cell type is 100. The cause of the normalization is to visualize the differences between Raman bands of three cell type.

As seen, there are several differences in the intensity of the bands appeared on the spectra. The tentative band assignments were listed in Table 1. The bands at 529, 667, 732, 797, 911, 964, 993, 1050, 1102, 1180, 1277, 1330, 1414, 1446, 1576 and 1654 cm^{-1} are visible in Figure 2.8.

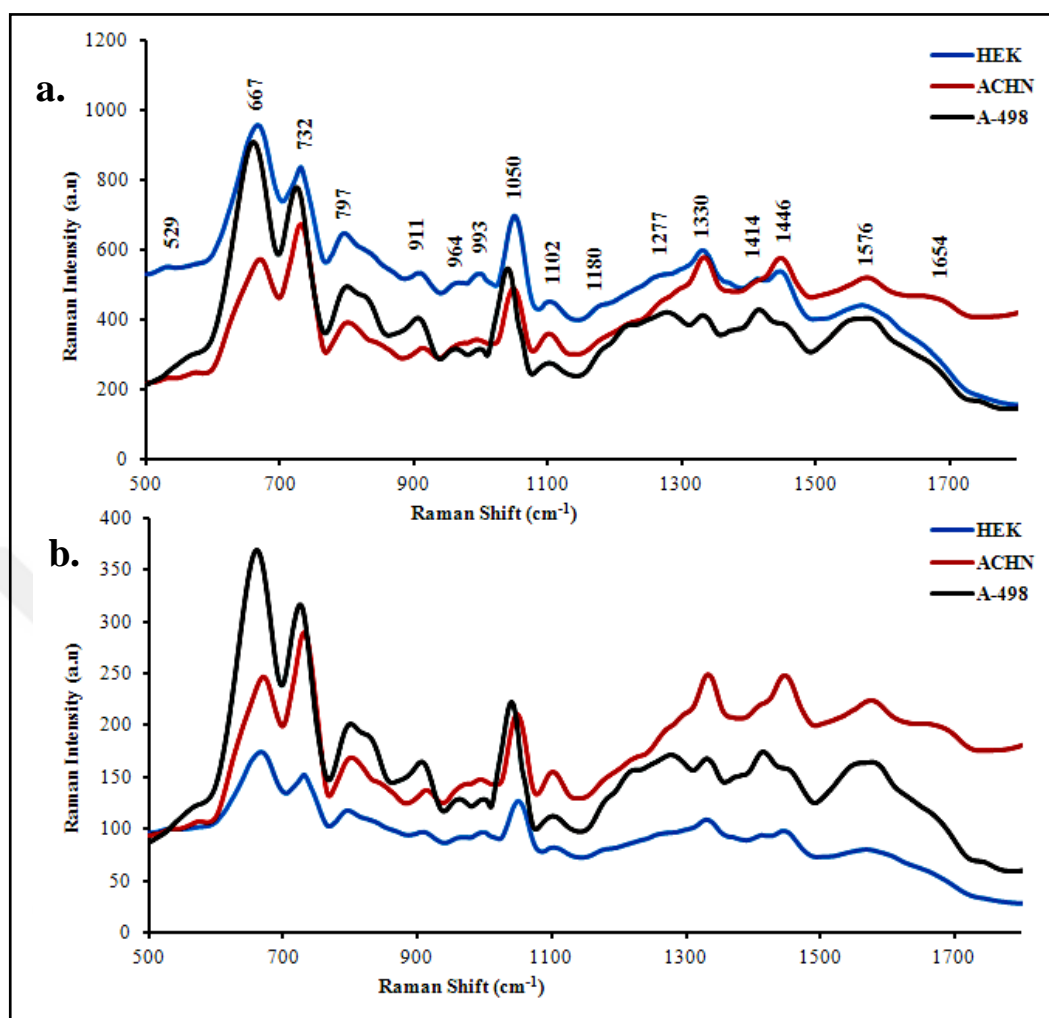


Figure 2.8. Mean SERS spectra from cultured cells; ACHN, A-498 and HEK 293. (a) Mean SERS spectra from HEK 293, a-498 and ACHN cultured cells. Spectra have been normalized to the intensity 529 cm^{-1} peak (b)

There is a strong Raman band around at 667 cm^{-1} for each cell lines. It is probably related to the presence of the sulphur atom: $\nu(\text{C-S})$ stretching causes intense bands in the region $600\text{--}700\text{ cm}^{-1}$. An important increase in the intensity of the band at 660 cm^{-1} in cancer cell lines is likely related to Glutathione (GSH) [121,122]. Glutathione is a tripeptide form of the amine group of cysteine and the carboxyl group of the glutamate side-chain. Cysteine is a sulfur-containing amino acid which can be found in natural foods and also produced by the body. Glutathione is found in all human tissues. It is an impressive antioxidant, protecting fatty tissues from hazardous effects of free radicals. The more intense bands obtained on SERS spectra of cancer cells can be interrelated with to conserve the lipid

conformation increased in cancer cells by Glutathione. The band at 732 cm^{-1} is recognized to nucleic acids and Phosphatidylserine, generally stored on the inner-leaflet of cell membranes [123]. Besides, the band at around 800 cm^{-1} on the spectra of the cancer cells is assigned to a benzene ring breathing vibration of tyrosine, which is more intense in cancer cells than the normal cells. This increase in protein concentration is established in cancer cells because of the high-energy demand for the increased metabolism. The band at around 906 cm^{-1} , which is more intense in cancer cells than healthy cells, is assigned to fatty acids and glucose. The anticipated decrease in the intensity of this band was observed on the spectra of HEK 293 cells compared to the spectra of the cancer cells. As a result, this decrease is a sign of the density of the phospholipids in the cancer cell membrane is higher. As the cell division is accelerated in cancer cells, they need to produce new cell membranes. Thus, the fatty acids production is increased. In addition, glucose, which is the primary source for energy is increased in cancer cells because the growth rate and proliferation is fast in cancer cells, and they require more energy than normal cell. The band at 964 cm^{-1} is recognized as malic acids, and the bands at 993 cm^{-1} is assigned as phenylalanine from proteins. The bands in region of $1000\text{-}1200\text{ cm}^{-1}$ originates from saccharides and fatty acids. The band in the region of $1200\text{-}1300\text{ cm}^{-1}$ defines proteins, including collagen I formation. The band examined at around 1300 cm^{-1} is broad for cancer cells while it is narrower for the healthy cells. The difference in the intensity of the bands at 529 , 1414 and 1446 cm^{-1} is assigned to saccharides, proteins and lipids. The band at 1446 cm^{-1} is more intense for healthy cells rather than cancer cells because phospholipids and glycerol are used more in metastatic cancer cells than healthy cells for cell adhesion during metastasis. In the region of $1500\text{-}1600\text{ cm}^{-1}$ are attributed to the pyrimidine ring of nucleotides and amide II bands. In addition, the Raman band at 1576 cm^{-1} , which assigned to Amide I is broader for A-498 cell line than the other cell lines but the intensity of the Raman band is higher for cancer cells than healthy cells.

Table 4.1. The band assignments of SERS spectra of the cell lines

Major assignments	Raman shift/ cm^{-1}		
	HEK	ACHN	A-498
Saccharides [124]	530	530	-
Phosphatidylinositol [125]	-	576	-
$\nu(\text{C-S})$ stretching [126]	668	670	660
Adenine (DNA/RNA) [127] / Phosphatidylserine [125]	732	732	725
RNA (PO_2 symmetric stretching) [128]/ tyrosine [129]	797	800	800
Fatty acids [130] / glucose [131]	911	914	906
Malic acid [124]	965	965	964
Phenylalanine [132]	993	993	998
Glycogen [133]/ fatty acids [124]	1050	1050	1040
Saccharides [134] / fatty acids [134]	1102	1102	1102
Cytosine and guanine [135]	1180	-	1180
Proteins [136], including collagen I	1278	1278	1278
Saccharides [137] /proteins [124]	1330	1333	1330
Fatty acids [124]/ saccharides [124]	1412	-	1414
Lipids [138]	1446	1447	1448
Amide II [139]/ DNA [140]	1577	1576	1577
Amide I [141]	-	1654	-

Further, the normalized SERS spectra were processed with MDS method by using SPSS (statistical package for the Social Sciences). MDS method generates distance matrixes, and it has the ability of the visualizing the relationship between cases, which are SERS spectra. The distance between the cells shows the similarity and dissimilarity. The 2D plots from the arbitrarily chosen 33 spectra obtained from each cell lines (a), and the 2D Euclidean distances plot of the one averaged spectra from 3000 SERS spectra for each cell line (b) were shown in Figure 2.9.

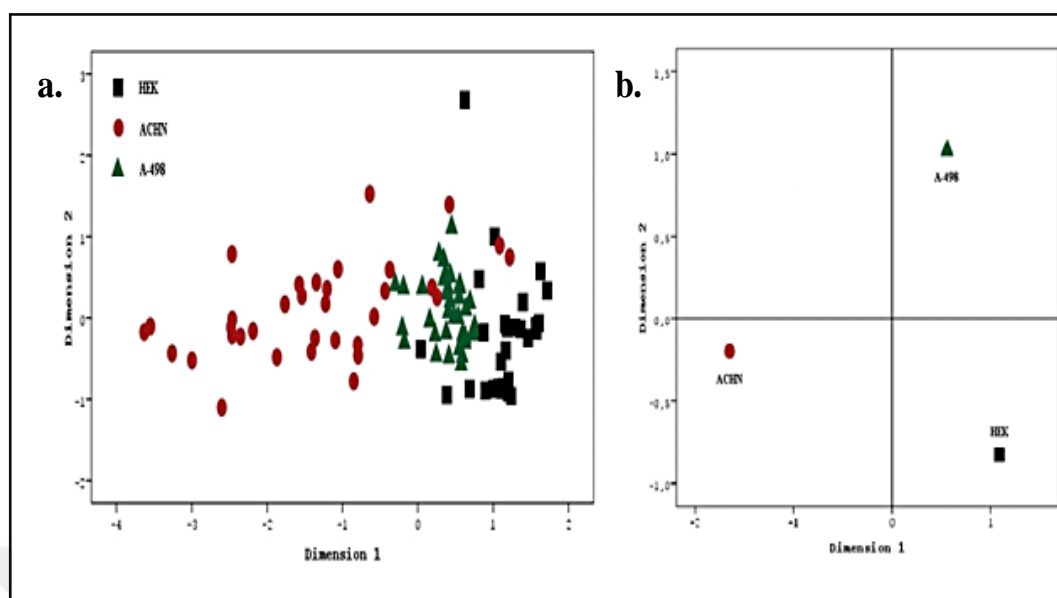


Figure 2.9. 2D Euclidean distances plot constructed from the arbitrarily chosen 33 spectra obtained from each cell lines (a), and 2D Euclidean distances plot of the one averaged spectra from 3000 SERS spectra for each cell line (b)

As seen in figure 4, HEK and A-498 cells are closely grouped according to their types, while the ACHN cells are placed farther than the other two. The cancer cells in high tumorigenicity have the ability of altering much faster than HEK, on-tumorigenic, and A-498, low tumorigenic.

MDS is not a correct solution and a subsequent technique on SERS data set because MDS is not an eigenvalue-eigenvector method while principal component analysis (PCA) is an eigenvalue-eigenvector method [142].

LDA, which is the classical discriminating method, are used in our study to obtain the differentiating of the cells in high efficiency. High dimensional SERS data set was reduced to principal component (PC) scores, new relevant variables. Four PC component eigenvectors were extracted, and PC 1 (44, 25% of the total variance), PC 2 (34, 51 %), PC 3 (13, 86 %) and PC 4 (2, 31 %) were graphed by using scatter plot to show the values of the three variables, ACHN, HEK and A-498 cell lines (Figure 5). Note that each dot represents one cell. The scatter plot of PC 1 and PC 2 was shown in figure 5 (A). As seen, PC 1 and PC 2 vectors could identify the cells with sensitivity and specificity of 85 %

and 84 %, respectively, while others are grouped in low correlation. PC 1 and PC 3 could classify the cell lines with sensitivity and specificity of 70 % and 68 %, respectively, while PC 1 and PC 4 could distinguish the cells with sensitivity and specificity of 70 % and 69 %, respectively. Besides, PC 2 and PC 3 could diagnose the three types of cells with sensitivity and specificity of 71 % and 69 %. In addition, PC 2 and PC 4 could differentiate the cell lines with sensitivity and specificity of 76 % and 73 %, respectively, while PC 3 and PC 4 could separate the cell lines with sensitivity and specificity of 46 % and 42 %, respectively.

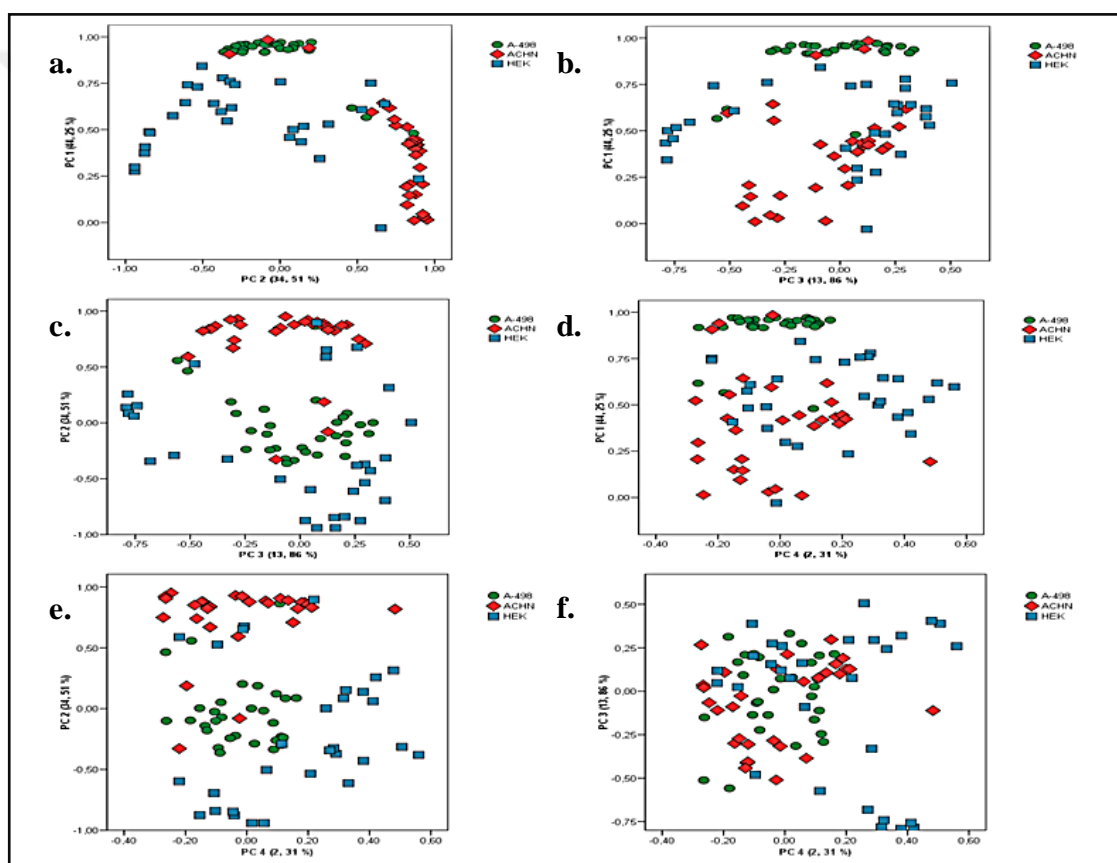


Figure 3.1. The PC scatter plots show the principal components of 30 cells from each cell lines (ACHN, A-498, and HEK 293). PC 1 and PC 2 (a), PC 1 and PC 3 (b), PC 2 and PC 3 (c), PC 1 and PC 4 (d), PC 2 and PC 4 (e), PC 3 and PC 4 (f)

PC 1 and PC 2 vectors have the large mean and significant differences between the groups compared to PC 3 and PC 4 vectors. As seen, it is clear that PCA is not the best classification methods for our SERS data set while it is a good way to summarize high data

sets into subsets of variables. LDA arranges discriminant functions by maximizing the variances in SERS data between different cell groups while minimizing the variances between the cells of the same group. The PC scores, reduced from high dimensional SERS data set were used in LDA. The scores on LD 1 and LD 2 were also graphed by using scatter plot (Figure 3.2). ACHN, HEK and A-498 cells are differentiated with sensitivity and specificity of 88 % and 84 % by LDA.

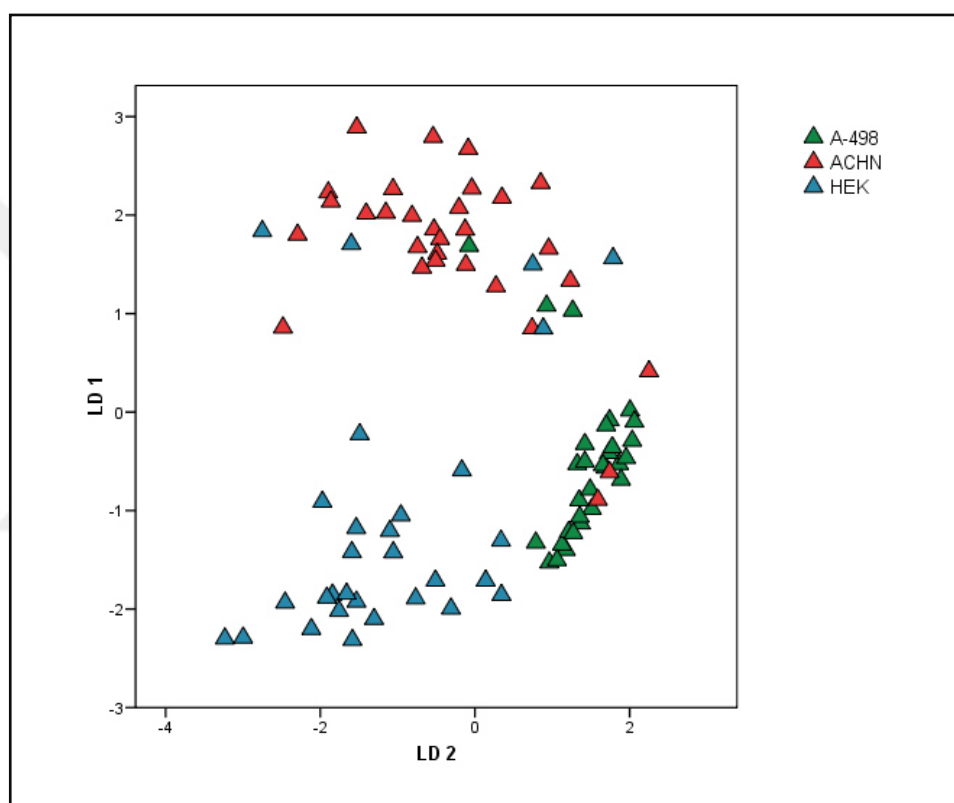


Figure3.2. LD 1 and LD 2 scatter plot of three types of cells

LDA is the best classification method for our study compared to PCA and MDS methods. As a result, the clustering of three cells with a sensitivity and specificity of 88 % and 84 %, respectively, is a good rate to diagnose of the cancer types of RCC and healthy cells. This study provides a novel approach for early detection of the RCC. The method is simple, label free and high classification rate compared to other SERS studies.

6. CONCLUSION AND RECOMMENDATIONS

6.1. CONCLUSION

In this study the use of SERS to identify renal cancer cells, human kidney adenocarcinoma (ACHN), human kidney carcinoma (A-498) and non-cancerous human kidney embryonic cells (HEK 293), by combining a new sampling method and LDA algorithms was demonstrated. The citrate reduced AgNPs were used as SERS substrates and the AgNPs colloidal suspension placed onto the cells grown on the slide was dried at the suspended position. Since the AgNPs and their aggregates are localized on the cell surface area with this sample preparation method, the observed bands on the SERS spectra of the cells can be attributed to the released metabolites or biomolecules originating from the cell surface and intra-cellular molecular molecules and molecular structures due to the cell rupture. The SERS spectra obtained from the three different cell lines are statistically analyzed to differentiate the cells. Principal component analysis (PCA) combined with linear discriminate analysis (LDA) was performed to differentiate the three kidney cell types with a sensitivity and specificity of 88 % and 84 %, respectively. The present study demonstrates that SERS can be used to differentiate renal cancers by combining a new sampling method and LDA algorithms. The observed changes on the SERS spectra can be related to altered biological function in healthy versus cancer cells, which could be used for early diagnosis or cell typing. This study was the first to differentiate the renal cancer cells from healthy cells with high correlation by using algorithms based PCA and LDA on SERS spectra set.

6.2. RECOMMENDATIONS

In this thesis, the development of a SERS based cell differentiation method was studied for three related cell lines. From the data presented here, it is evidenced that the approach can be used for the cell differentiation. However, it is necessary to conduct further studies if the developed approach is efficient for the differentiation of all types of cells.

Another interesting future study can be the use of modified AgNPs by introducing them into the cells other than placing them onto the cells. Although there are studies in literature employing mostly the AuNPs, there are not many reports that the AgNPs are used. The possible reason for this could be the toxicity of the AgNPs to the living cells. The modification of the AgNPs with biocompatible molecules and polymers can be used to diminish their toxicity for living cells. In addition, with the attachment of receptor molecules such antibodies, specific target molecules can be captured in living cells.

Further, the SERS spectra obtained from the cell lines can be compared to the SERS spectra obtained from the cancer tissue using a similar statistical approach for a possible use of the developed approach for diagnosis.

7. REFERENCES

1. Fass, L., "Imaging and cancer: a review", *Molecular oncology*, Vol. 2, pp. 115-152, 2008.
2. Gao, X., Cui, Y., Levenson, R. M., Chung, L. W., Nie, S., "In vivo cancer targeting and imaging with semiconductor quantum dots", *Nature biotechnology*, Vol. 22, pp. 969-976, 2004.
3. Lakowicz, J. R., *Principles of fluorescence spectroscopy*, Springer, 2009.
4. Lin-Vien, D., *The Handbook of infrared and Raman characteristic frequencies of organic molecules*, Academic Press, 1991.
5. Colthup, N., Daly, L., Wiberley, S., "Introduction to infrared and raman spectroscopy POD", 1990.
6. Alfano, R. R., Liu, C. H., Glassman, W. S., "Method for determining if a tissue is a malignant tumor tissue, a benign tumor tissue, or a normal or benign tissue using Raman spectroscopy", Google Patents, 1993.
7. Aydin, Ö., Altaş, M., Kahraman, M., Bayrak, Ö. F., Çulha, M., "Differentiation of healthy brain tissue and tumors using surface-enhanced Raman scattering", *Applied spectroscopy*, Vol. 63, pp. 1095-1100, 2009.
8. Aydin, Ö., Kahraman, M., Kiliç, E., Çulha, M., "Surface-enhanced Raman scattering of rat tissues", *Applied spectroscopy*, Vol. 63, pp. 662-668, 2009.
9. Petry, R., Schmitt, M., Popp, J., "Raman spectroscopy—a prospective tool in the life sciences", *ChemPhysChem*, Vol. 4, pp. 14-30, 2003.

10. Kendall, C., Stone, N., Shepherd, N., Geboes, K., Warren, B., Bennett, R., Barr, H., "Raman spectroscopy, a potential tool for the objective identification and classification of neoplasia in Barrett's oesophagus", *The Journal of pathology*, Vol. 200, pp. 602-609, 2003.
11. Yu, C., Gestl, E., Eckert, K., Allara, D., Irudayaraj, J., "Characterization of human breast epithelial cells by confocal Raman microspectroscopy", *Cancer detection and prevention*, Vol. 30, pp. 515-522, 2006.
12. Lyng, F. M., Faoláin, E. Ó., Conroy, J., Meade, A., Knief, P., Duffy, B., Hunter, M., Byrne, J., Kelehan, P., Byrne, H. J., "Vibrational spectroscopy for cervical cancer pathology, from biochemical analysis to diagnostic tool", *Experimental and molecular pathology*, Vol. 82, pp. 121-129, 2007.
13. Feng, S., Chen, R., Lin, J., Pan, J., Chen, G., Li, Y., Cheng, M., Huang, Z., Chen, J., Zeng, H., "Nasopharyngeal cancer detection based on blood plasma surface-enhanced Raman spectroscopy and multivariate analysis", *Biosensors and Bioelectronics*, Vol. 25, pp. 2414-2419, 2010.
14. Qian, X., Peng, X.-H., Ansari, D. O., Yin-Goen, Q., Chen, G. Z., Shin, D. M., Yang, L., Young, A. N., Wang, M. D., Nie, S., "In vivo tumor targeting and spectroscopic detection with surface-enhanced Raman nanoparticle tags", *Nature biotechnology*, Vol. 26, pp. 83-90, 2007.
15. Sigurdsson, S., Philipsen, P. A., Hansen, L. K., Larsen, J., Gniadecka, M., Wulf, H. C., "Detection of skin cancer by classification of Raman spectra", *Biomedical Engineering, IEEE Transactions on*, Vol. 51, pp. 1784-1793, 2004.
16. Kneipp, K., Moskovits, M., Kneipp, H., *Surface-enhanced Raman scattering: physics and applications*, Springer, 2006.

17. Kneipp, K., Kneipp, H., Kartha, V. B., Manoharan, R., Deinum, G., Itzkan, I., Dasari, R. R., Feld, M. S., "Detection and identification of a single DNA base molecule using surface-enhanced Raman scattering (SERS)", *Physical Review E*, Vol. 57, pp. R6281-R6284, 1998.
18. Wang, Y., Wei, H., Li, B., Ren, W., Guo, S., Dong, S., Wang, E., "SERS opens a new way in aptasensor for protein recognition with high sensitivity and selectivity", *Chemical Communications*, pp. 5220-5222, 2007.
19. Premasiri, W., Moir, D., Klempner, M., Krieger, N., Jones, G., Ziegler, L., "Characterization of the surface enhanced Raman scattering (SERS) of bacteria", *The Journal of Physical Chemistry B*, Vol. 109, pp. 312-320, 2005.
20. Kneipp, K., Haka, A. S., Kneipp, H., Badizadegan, K., Yoshizawa, N., Boone, C., Shafer-Peltier, K. E., Motz, J. T., Dasari, R. R., Feld, M. S., "Surface-enhanced Raman spectroscopy in single living cells using gold nanoparticles", *Applied spectroscopy*, Vol. 56, pp. 150-154, 2002.
21. Nabiev, I., Morjani, H., Manfait, M., "Selective analysis of antitumor drug interaction with living cancer cells as probed by surface-enhanced Raman spectroscopy", *European biophysics journal*, Vol. 19, pp. 311-316, 1991.
22. Breuzard, G., Angiboust, J. F., Jeannesson, P., Manfait, M., Millot, J. M., "Surface-enhanced Raman scattering reveals adsorption of mitoxantrone on plasma membrane of living cells", *Biochemical and Biophysical Research Communications*, Vol. 320, pp. 615-621, 2004.
23. Eliasson, C., Lorén, A., Engelsektsson, J., Josefson, M., Abrahamsson, J., Abrahamsson, K., "Surface-enhanced Raman scattering imaging of single living lymphocytes with multivariate evaluation", *Spectrochimica Acta Part A: Molecular and Biomolecular Spectroscopy*, Vol. 61, pp. 755-760, 2005.

24. Huang, X., El-Sayed, I. H., Qian, W., El-Sayed, M. A., "Cancer cell imaging and photothermal therapy in the near-infrared region by using gold nanorods", *Journal of the American Chemical Society*, Vol. 128, pp. 2115-2120, 2006.
25. Huang, X., El-Sayed, I. H., Qian, W., El-Sayed, M. A., "Cancer cells assemble and align gold nanorods conjugated to antibodies to produce highly enhanced, sharp, and polarized surface Raman spectra: a potential cancer diagnostic marker", *Nano letters*, Vol. 7, pp. 1591-1597, 2007.
26. Kim, J.-H., Kim, J.-S., Choi, H., Lee, S.-M., Jun, B.-H., Yu, K.-N., Kuk, E., Kim, Y.-K., Jeong, D. H., Cho, M.-H., "Nanoparticle probes with surface enhanced Raman spectroscopic tags for cellular cancer targeting", *Analytical Chemistry*, Vol. 78, pp. 6967-6973, 2006.
27. Kneipp, K., Kneipp, H., Kneipp, J., "Surface-enhanced Raman scattering in local optical fields of silver and gold nanoaggregates from single-molecule Raman spectroscopy to ultrasensitive probing in live cells", *Accounts of chemical research*, Vol. 39, pp. 443-450, 2006.
28. Shanmukh, S., Jones, L., Driskell, J., Zhao, Y., Dluhy, R., Tripp, R. A., "Rapid and sensitive detection of respiratory virus molecular signatures using a silver nanorod array SERS substrate", *Nano Letters*, Vol. 6, pp. 2630-2636, 2006.
29. Vo-Dinh, T., Allain, L. R., Stokes, D. L., "Cancer gene detection using surface-enhanced Raman scattering (SERS)", *Journal of Raman Spectroscopy*, Vol. 33, pp. 511-516, 2002.
30. Wang, Z., Bonoiu, A., Samoc, M., Cui, Y., Prasad, P. N., "Biological pH sensing based on surface enhanced Raman scattering through a 2-aminothiophenol-silver probe", *Biosensors and Bioelectronics*, Vol. 23, pp. 886-891, 2008.

31. Xie, W., Wang, L., Zhang, Y., Su, L., Shen, A., Tan, J., Hu, J., "Nuclear targeted nanoprobe for single living cell detection by surface-enhanced Raman scattering", *Bioconjugate chemistry*, Vol. 20, pp. 768-773, 2009.
32. Siegel, R., Naishadham, D., Jemal, A., "Cancer statistics, 2012", *CA: a cancer journal for clinicians*, Vol. 62, pp. 10-29, 2012.
33. Chow, W.-H., Dong, L. M., Devesa, S. S., "Epidemiology and risk factors for kidney cancer", *Nature Reviews Urology*, Vol. 7, pp. 245-257, 2010.
34. Ljungberg, B., Hanbury, D. C., Kuczyk, M. A., Merseburger, A. S., Mulders, P. F., Patard, J.-J., Sinescu, I. C., "Renal cell carcinoma guideline", *European urology*, Vol. 51, pp. 1502-1510, 2007.
35. Black, W. C., Welch, H. G., "Advances in diagnostic imaging and overestimations of disease prevalence and the benefits of therapy", *New England Journal of Medicine*, Vol. 328, pp. 1237-1243, 1993.
36. Carroll, J. D., Chang, J.-J., "Analysis of individual differences in multidimensional scaling via an N-way generalization of "Eckart-Young" decomposition", *Psychometrika*, Vol. 35, pp. 283-319, 1970.
37. Keskin, S., Çulha, M., "Label-free detection of proteins from dried-suspended droplets using surface enhanced Raman scattering", *The Analyst*, Vol. 137, pp. 2651, 2012.
38. Larkin, P. J., Scowcroft, W., "Somaclonal variation—a novel source of variability from cell cultures for plant improvement", *Theoretical and Applied Genetics*, Vol. 60, pp. 197-214, 1981.
39. Carpita, N. C., Gibeaut, D. M., "Structural models of primary cell walls in flowering plants: consistency of molecular structure with the physical properties of the walls during growth", *The Plant Journal*, Vol. 3, pp. 1-30, 1993.

40. Dijksterhuis, J., Nijse, J., Hoekstra, F., Golovina, E., "High viscosity and anisotropy characterize the cytoplasm of fungal dormant stress-resistant spores", *Eukaryotic cell*, Vol. 6, pp. 157-170, 2007.
41. Bevan, M. W., Flavell, R. B., Chilton, M.-D., "A chimaeric antibiotic resistance gene as a selectable marker for plant cell transformation", 1983.
42. Schenk, R. U., Hildebrandt, A., "Medium and techniques for induction and growth of monocotyledonous and dicotyledonous plant cell cultures", *Canadian Journal of Botany*, Vol. 50, pp. 199-204, 1972.
43. Showalter, A. M., "Structure and function of plant cell wall proteins", *The Plant Cell*, Vol. 5, pp. 9, 1993.
44. Preston, R. D., *The physical biology of plant cell walls*, London.: Chapman & Hall, 1974.
45. Parkin, D. M., Bray, F., Ferlay, J., Pisani, P., "Global cancer statistics, 2002", *CA: a cancer journal for clinicians*, Vol. 55, pp. 74-108, 2005.
46. Parkin, D. M., "Global cancer statistics in the year 2000", *The lancet oncology*, Vol. 2, pp. 533-543, 2001.
47. Kushi, L. H., Byers, T., Doyle, C., Bandera, E. V., McCullough, M., Gansler, T., Andrews, K. S., Thun, M. J., "American Cancer Society Guidelines on Nutrition and Physical Activity for cancer prevention: reducing the risk of cancer with healthy food choices and physical activity", *CA: a cancer journal for clinicians*, Vol. 56, pp. 254-281, 2006.
48. Smith, R. A., Cokkinides, V., Eyre, H. J., "American Cancer Society guidelines for the early detection of cancer, 2004", *CA: a cancer journal for clinicians*, Vol. 54, pp. 41-52, 2004.

49. Begg, A. C., Stewart, F. A., Vens, C., "Strategies to improve radiotherapy with targeted drugs", *Nature Reviews Cancer*, Vol. 11, pp. 239-253, 2011.
50. Richardson, J. L., Marks, G., Levine, A., "The influence of symptoms of disease and side effects of treatment on compliance with cancer therapy", *Journal of Clinical Oncology*, Vol. 6, pp. 1746-1752, 1988.
51. Scappaticci, F. A., "Mechanisms and future directions for angiogenesis-based cancer therapies", *Journal of Clinical Oncology*, Vol. 20, pp. 3906-3927, 2002.
52. Kreidberg, J. A., Sariola, H., Loring, J. M., Maeda, M., Pelletier, J., Housman, D., Jaenisch, R., "WT-1 is required for early kidney development", *Cell*, Vol. 74, pp. 679-691, 1993.
53. Parkin, D. M., Pisani, P., Ferlay, J., "Global cancer statistics", *CA: a cancer journal for clinicians*, Vol. 49, pp. 33-64, 1999.
54. Jemal, A., Siegel, R., Ward, E., Murray, T., Xu, J., Thun, M. J., "Cancer statistics, 2007", *CA: a cancer journal for clinicians*, Vol. 57, pp. 43-66, 2007.
55. Pischon, T., Lahmann, P. H., Boeing, H., Tjønneland, A., Halkjær, J., Overvad, K., Klipstein-Grobusch, K., Linseisen, J., Becker, N., Trichopoulou, A., "Body size and risk of renal cell carcinoma in the European Prospective Investigation into Cancer and Nutrition (EPIC)", *International journal of cancer*, Vol. 118, pp. 728-738, 2006.
56. Rini, B. I., Campbell, S. C., Escudier, B., "Renal cell carcinoma", *The Lancet*, Vol. 373, pp. 1119-1132, 2009.
57. Lam, J. S., Leppert, J. T., Figlin, R. A., Belldegrun, A. S., "Role of molecular markers in the diagnosis and therapy of renal cell carcinoma", *Urology*, Vol. 66, pp. 1-9, 2005.

58. Crespy, G., "Spontaneous recovery from metastatic cancer of the kidney. Favourable role of Vitamin E?]", *Journal de chirurgie*, Vol. 130, pp. 470, 1993.
59. Ferraro, J. R., *Introductory raman spectroscopy*, Academic press, 2003.
60. Perchard, J., Murphy, W., Bernstein, H., "Raman and Rayleigh spectroscopy and molecular motions: I. Liquid hydrochloric and hydrobromic acids and their deuterated analogues† Issued as NRCC 12632", *Molecular Physics*, Vol. 23, pp. 499-517, 1972.
61. Demtröder, W., "Laser spectroscopy: basic concepts and instrumentation", *NASA STI/Recon Technical Report A*, Vol. 82, pp. 12273, 1981.
62. Cao, Y. C., Jin, R., Mirkin, C. A., "Nanoparticles with Raman spectroscopic fingerprints for DNA and RNA detection", *Science*, Vol. 297, pp. 1536-1540, 2002.
63. Fleischmann, M., Hendra, P., McQuillan, A., "Raman spectra of pyridine adsorbed at a silver electrode", *Chemical Physics Letters*, Vol. 26, pp. 163-166, 1974.
64. Jeanmaire, D. L., Van Duyne, R. P., "Surface Raman spectroelectrochemistry: Part I. Heterocyclic, aromatic, and aliphatic amines adsorbed on the anodized silver electrode", *Journal of Electroanalytical Chemistry and Interfacial Electrochemistry*, Vol. 84, pp. 1-20, 1977.
65. Albrecht, M. G., Creighton, J. A., "Anomalously intense Raman spectra of pyridine at a silver electrode", *Journal of the American Chemical Society*, Vol. 99, pp. 5215-5217, 1977.
66. Barnes, W. L., Dereux, A., Ebbesen, T. W., "Surface plasmon subwavelength optics", *Nature*, Vol. 424, pp. 824-830, 2003.

67. Murphy, C. J., Sau, T. K., Gole, A. M., Orendorff, C. J., Gao, J., Gou, L., Hunyadi, S. E., Li, T., "Anisotropic metal nanoparticles: synthesis, assembly, and optical applications", *The Journal of Physical Chemistry B*, Vol. 109, pp. 13857-13870, 2005.
68. Zhang, J., Li, X., Sun, X., Li, Y., "Surface enhanced Raman scattering effects of silver colloids with different shapes", *The Journal of Physical Chemistry B*, Vol. 109, pp. 12544-12548, 2005.
69. Rivas, L., Sanchez-Cortes, S., Garcia-Ramos, J., Morcillo, G., "Mixed silver/gold colloids: a study of their formation, morphology, and surface-enhanced Raman activity", *Langmuir*, Vol. 16, pp. 9722-9728, 2000.
70. Lee, P., Meisel, D., "Adsorption and surface-enhanced Raman of dyes on silver and gold sols", *The Journal of Physical Chemistry*, Vol. 86, pp. 3391-3395, 1982.
71. Youda, R., Nishihara, H., Aramaki, K., "SERS and impedance study of the equilibrium between complex formation and adsorption of benzotriazole and 4-hydroxybenzotriazole on a copper electrode in sulphate solutions", *Electrochimica acta*, Vol. 35, pp. 1011-1017, 1990.
72. Abdelsalam, M. E., Mahajan, S., Bartlett, P. N., Baumberg, J. J., Russell, A. E., "SERS at structured palladium and platinum surfaces", *Journal of the American Chemical Society*, Vol. 129, pp. 7399-7406, 2007.
73. Xiong, Y., McLellan, J. M., Chen, J., Yin, Y., Li, Z.-Y., Xia, Y., "Kinetically controlled synthesis of triangular and hexagonal nanoplates of palladium and their SPR/SERS properties", *Journal of the American Chemical Society*, Vol. 127, pp. 17118-17127, 2005.

74. Creighton, J., "Surface Raman electromagnetic enhancement factors for molecules at the surface of small isolated metal spheres: The determination of adsorbate orientation from SERS relative intensities", *Surface Science*, Vol. 124, pp. 209-219, 1983.
75. Kneipp, K., Kneipp, H., Itzkan, I., Dasari, R. R., Feld, M. S., "Surface-enhanced Raman scattering and biophysics", *Journal of Physics: Condensed Matter*, Vol. 14, pp. R597, 2002.
76. Volkan, M., Stokes, D. L., Vo-Dinh, T., "Surface-enhanced Raman of dopamine and neurotransmitters using sol-gel substrates and polymer-coated fiber-optic probes", *Applied spectroscopy*, Vol. 54, pp. 1842-1848, 2000.
77. YuláLim, S., JináKim, B., DongáChung, T., "Mercury (II) detection by SERS based on a single gold microshell", *Chemical Communications*, Vol. 46, pp. 5587-5589, 2010.
78. Weldon, M. K., Zhelyaskov, V. R., Morris, M. D., "Surface-enhanced Raman spectroscopy of lipids on silver microprobes", *Applied spectroscopy*, Vol. 52, pp. 265-269, 1998.
79. Leopold, N., Lendl, B., "A new method for fast preparation of highly surface-enhanced Raman scattering (SERS) active silver colloids at room temperature by reduction of silver nitrate with hydroxylamine hydrochloride", *The Journal of Physical Chemistry B*, Vol. 107, pp. 5723-5727, 2003.
80. Kabashin, A., Meunier, M., "Synthesis of colloidal nanoparticles during femtosecond laser ablation of gold in water", *Journal of applied physics*, Vol. 94, pp. 7941-7943, 2003.
81. Mafuné, F., Kohno, J.-y., Takeda, Y., Kondow, T., "Full physical preparation of size-selected gold nanoparticles in solution: laser ablation and laser-induced size control", *The Journal of Physical Chemistry B*, Vol. 106, pp. 7575-7577, 2002.

82. Ji, X., Song, X., Li, J., Bai, Y., Yang, W., Peng, X., "Size control of gold nanocrystals in citrate reduction: the third role of citrate", *Journal of the American Chemical Society*, Vol. 129, pp. 13939-13948, 2007.
83. Aslam, M., Fu, L., Su, M., Vijayamohan, K., Dravid, V. P., "Novel one-step synthesis of amine-stabilized aqueous colloidal gold nanoparticles", *Journal of Materials Chemistry*, Vol. 14, pp. 1795-1797, 2004.
84. Cotton, T. M., Kim, J. H., Chumanov, G. D., "Application of surface-enhanced Raman spectroscopy to biological systems", *Journal of Raman Spectroscopy*, Vol. 22, pp. 729-742, 1991.
85. Koglin, E., Séquaris, J.-M., "Surface enhanced Raman scattering of biomolecules", in *Analytical Problems*, pp. 1-57, Springer, 1986.
86. Rohr, T. E., Cotton, T., Fan, N., Tarcha, P. J., "Immunoassay employing surface-enhanced Raman spectroscopy", *Analytical biochemistry*, Vol. 182, pp. 388-398, 1989.
87. Zhelyaskov, V. R., Milne, E. T., Hetke, J. F., Morris, M. D., "Silicon substrate microelectrode array for surface-enhanced Raman spectroscopy", *Applied spectroscopy*, Vol. 49, pp. 1793-1795, 1995.
88. Dou, X., Takama, T., Yamaguchi, Y., Yamamoto, H., Ozaki, Y., "Enzyme immunoassay utilizing surface-enhanced Raman scattering of the enzyme reaction product", *Analytical chemistry*, Vol. 69, pp. 1492-1495, 1997.
89. Nascimento, F. C., Carneiro, C. E., de Santana, H., Zaia, D. A., "The Effect of Artificial Seawater on SERS Spectra of Amino Acids-Ag Colloids: an Experiment of Prebiotic Chemistry", *Spectrochimica Acta Part A: Molecular and Biomolecular Spectroscopy*, 2013.

90. Li, P., Zhou, X., Liu, H., Yang, L., Liu, J., "Surface-enhanced Raman evidence for Rhodamine 6 G and its derivative with different adsorption geometry to colloidal silver nanoparticle", *Journal of Raman Spectroscopy*, 2013.
91. Wiechen, K., Diatchenko, L., Agoulnik, A., Scharff, K. M., Schober, H., Arlt, K., Zhumabayeva, B., Siebert, P. D., Dietel, M., Schäfer, R., "Caveolin-1 Is Down-Regulated in Human Ovarian Carcinoma and Acts as a Candidate Tumor Suppressor Gene", *The American journal of pathology*, Vol. 159, pp. 1635-1643, 2001.
92. Suh, J., Moskovits, M., "Surface-enhanced Raman spectroscopy of amino acids and nucleotide bases adsorbed on silver", *Journal of the American Chemical Society*, Vol. 108, pp. 4711-4718, 1986.
93. Peng, C., Buldyrev, S., Goldberger, A., Havlin, S., Sciortino, F., Simons, M., Stanley, H., "Long-range correlations in nucleotide sequences", *Nature*, Vol. 356, pp. 168-170, 1992.
94. Li, W., Godzik, A., "Cd-hit: a fast program for clustering and comparing large sets of protein or nucleotide sequences", *Bioinformatics*, Vol. 22, pp. 1658-1659, 2006.
95. Chen, Z., Tabakman, S. M., Goodwin, A. P., Kattah, M. G., Daranciang, D., Wang, X., Zhang, G., Li, X., Liu, Z., Utz, P. J., "Protein microarrays with carbon nanotubes as multicolor Raman labels", *Nature biotechnology*, Vol. 26, pp. 1285-1292, 2008.
96. Bell, S. E., Sirimuthu, N. M., "Surface-enhanced Raman spectroscopy (SERS) for sub-micromolar detection of DNA/RNA mononucleotides", *Journal of the American Chemical Society*, Vol. 128, pp. 15580-15581, 2006.

97. Kneipp, K., Kneipp, H., Kartha, V. B., Manoharan, R., Deinum, G., Itzkan, I., Dasari, R. R., Feld, M. S., "Detection and identification of a single DNA base molecule using surface-enhanced Raman scattering (SERS)", *Physical Review E*, Vol. 57, pp. R6281, 1998.
98. Thomas, L. L., Kim, J. H., Cotton, T. M., "Comparative study of resonance Raman and surface-enhanced resonance Raman chlorophyll a spectra using solet and red excitation", *Journal of the American Chemical Society*, Vol. 112, pp. 9378-9386, 1990.
99. Sánchez-Cortés, S., Miskovsky, P., Jancura, D., Bertoluzza, A., "Specific interactions of antiretrovirally active drug hypericin with DNA as studied by surface-enhanced resonance Raman spectroscopy", *The Journal of Physical Chemistry*, Vol. 100, pp. 1938-1944, 1996.
100. Wood, E., Sutton, C., Beezer, A., Creighton, J., Davis, A., Mitchell, J., "Surface enhanced Raman scattering (SERS) study of membrane transport processes", *Int. J. Pharm.*, Vol. 154, pp. 115-118, 1997.
101. Tracewell, C. A., Vrettos, J. S., Bautista, J. A., Frank, H. A., Brudvig, G. W., "Carotenoid photooxidation in photosystem II", *Archives of Biochemistry and Biophysics*, Vol. 385, pp. 61-69, 2001.
102. Efrima, S., Bronk, B., "Silver colloids impregnating or coating bacteria", *The Journal of Physical Chemistry B*, Vol. 102, pp. 5947-5950, 1998.
103. Beljebbar, A., Sockalingum, G. D., Morjani, H., Manfait, M., "presented" at the *BiOS'99 International Biomedical Optics Symposium*, 1999 (unpublished).
104. Ganbold, E. O., Byun, J., Lee, S., Joo, S. W., "Raman spectroscopy of combinatory anticancer drug release from gold nanoparticles inside a single leukemia cell", *Journal of Raman Spectroscopy*, 2013.

105. Hodges, M. D., Kelly, J. G., Bentley, A. J., Fogarty, S., Patel, I. I., Martin, F. L., Fullwood, N. J., "Combining immunolabeling and surface-enhanced Raman spectroscopy on cell membranes", *ACS Nano*, Vol. 5, pp. 9535-9541, 2011.
106. Jiang, X., Jiang, Z., Xu, T., Su, S., Zhong, Y., Peng, F., Su, Y., He, Y., "SERS-Based Sensing in Vitro: Facile and Label-Free Detection of Apoptotic Cells at the Single-Cell Level", *Analytical chemistry*, 2013.
107. Lin, J., Chen, R., Feng, S., Li, Y., Huang, Z., Xie, S., Yu, Y., Cheng, M., Zeng, H., "Rapid delivery of silver nanoparticles into living cells by electroporation for surface-enhanced Raman spectroscopy", *Biosensors and Bioelectronics*, Vol. 25, pp. 388-394, 2009.
108. Sockalingum, G., Beljebbar, A., Morjani, H., Angiboust, J., Manfait, M., "Characterization of island films as surface-enhanced Raman spectroscopy substrates for detecting low antitumor drug concentrations at single cell level", *Biospectroscopy*, Vol. 4, pp. S71-S78, 1998.
109. Huh, Y. S., Chung, A. J., Erickson, D., "Surface enhanced Raman spectroscopy and its application to molecular and cellular analysis", *Microfluidics and nanofluidics*, Vol. 6, pp. 285-297, 2009.
110. Sujith, A., Itoh, T., Abe, H., Yoshida, K.-i., Kiran, M. S., Biju, V., Ishikawa, M., "Imaging the cell wall of living single yeast cells using surface-enhanced Raman spectroscopy", *Analytical and bioanalytical chemistry*, Vol. 394, pp. 1803-1809, 2009.
111. Breuzard, G., Angiboust, J.-F., Jeannesson, P., Manfait, M., Millot, J.-M., "Surface-enhanced Raman scattering reveals adsorption of mitoxantrone on plasma membrane of living cells", *Biochemical and biophysical research communications*, Vol. 320, pp. 615-621, 2004.

112. hn, M. A., Jess, P. R., Stoquert, H., Dholakia, K., Campbell, C. J., "Nanoshells for surface-enhanced Raman spectroscopy in eukaryotic cells: cellular response and sensor development", *ACS nano*, Vol. 3, pp. 3613-3621, 2009.
113. Wang, Y., Li, D., Li, P., Wang, W., Ren, W., Dong, S., Wang, E., "Surface enhanced Raman scattering of brilliant green on Ag nanoparticles and applications in living cells as optical probes", *The Journal of Physical Chemistry C*, Vol. 111, pp. 16833-16839, 2007.
114. Li, M., Yuan, B., "2D-LDA: A statistical linear discriminant analysis for image matrix", *Pattern Recognition Letters*, Vol. 26, pp. 527-532, 2005.
115. Jolliffe, I., *Principal component analysis*, Wiley Online Library, 2005.
116. Shen, X., Ho, C.-M., Wong, T.-S., "Minimal size of coffee ring structure", *The Journal of Physical Chemistry B*, Vol. 114, pp. 5269-5274, 2010.
117. Hu, H., Larson, R. G., "Marangoni effect reverses coffee-ring depositions", *The Journal of Physical Chemistry B*, Vol. 110, pp. 7090-7094, 2006.
118. Jiang, J., Bosnick, K., Maillard, M., Brus, L., "Single molecule Raman spectroscopy at the junctions of large Ag nanocrystals", *The Journal of Physical Chemistry B*, Vol. 107, pp. 9964-9972, 2003.
119. Safonov, V., Shalaev, V., Markel, V., Danilova, Y. E., Lepeshkin, N., Kim, W., Rautian, S., Armstrong, R., "Spectral dependence of selective photomodification in fractal aggregates of colloidal particles", *Physical review letters*, Vol. 80, pp. 1102, 1998.
120. Kneipp, K., Kneipp, H., Corio, P., Brown, S., Shafer, K., Motz, J., Perelman, L., Hanlon, E., Marucci, A., Dresselhaus, G., "Surface-enhanced and normal stokes and anti-stokes Raman spectroscopy of single-walled carbon nanotubes", *Physical review letters*, Vol. 84, pp. 3470, 2000.

121. Quintana-Cabrera, R., Bolaños, J., "Glutathione and γ -glutamylcysteine in the antioxidant and survival functions of mitochondria", *Biochemical Society transactions*, Vol. 41, pp. 106-110, 2013.
122. Kumar, P., Maurya, P. K., "L-cysteine efflux in erythrocytes as a function of human age: correlation with reduced glutathione and total antioxidant potential", *Rejuvenation research*, 2013.
123. Blankenberg, F. G., Katsikis, P. D., Tait, J. F., Davis, R. E., Naumovski, L., Ohtsuki, K., Kopywoda, S., Abrams, M. J., Darkes, M., Robbins, R. C., "In vivo detection and imaging of phosphatidylserine expression during programmed cell death", *Proceedings of the National Academy of Sciences*, Vol. 95, pp. 6349-6354, 1998.
124. De Gelder, J., De Gussem, K., Vandenabeele, P., Moens, L., "Reference database of Raman spectra of biological molecules", *Journal of Raman Spectroscopy*, Vol. 38, pp. 1133-1147, 2007.
125. Movasaghi, Z., Rehman, S., Rehman, I. U., "Raman spectroscopy of biological tissues", *Applied Spectroscopy Reviews*, Vol. 42, pp. 493-541, 2007.
126. Bastian Jr, E. J., Martin, R. B., "Disulfide vibrational spectra in the sulfur-sulfur and carbon-sulfur stretching region", *The Journal of Physical Chemistry*, Vol. 77, pp. 1129-1133, 1973.
127. Katahira, M., Nishimura, Y., Tsuboi, M., Sato, T., Mitsui, Y., Iitaka, Y., "Local and overall conformations of DNA double helices with the A·T base pairs", *Biochimica et Biophysica Acta (BBA)-Gene Structure and Expression*, Vol. 867, pp. 256-267, 1986.
128. Lafleur, L., Rice, J., Thomas, G., "Raman studies of nucleic acids. VII. Poly A·poly U and poly G·Poly C", *Biopolymers*, Vol. 11, pp. 2423-2437, 1972.

129. Ravikumar, B., Rajaram, R., Ramakrishnan, V., "Raman and IR spectral studies of Lphenylalanine Lphenylalaninium dihydrogenphosphate and DLphenylalaninium dihydrogenphosphate", *Journal of Raman Spectroscopy*, Vol. 37, pp. 597-605, 2006.
130. Vandenabeele, P., Wehling, B., Moens, L., Edwards, H., De Reu, M., Van Hooydonk, G., "Analysis with micro-Raman spectroscopy of natural organic binding media and varnishes used in art", *Analytica Chimica Acta*, Vol. 407, pp. 261-274, 2000.
131. Vasko, P., Blackwell, J., Koenig, J., "Infrared and raman spectroscopy of carbohydrates.: Part II: Normal coordinate analysis of α -D-glucose", *Carbohydrate Research*, Vol. 23, pp. 407-416, 1972.
132. Frushour, B. G., Koenig, J. L., "Raman scattering of collagen, gelatin, and elastin", *Biopolymers*, Vol. 14, pp. 379-391, 1975.
133. Wong, P., Wong, R. K., Caputo, T. A., Godwin, T. A., Rigas, B., "Infrared spectroscopy of exfoliated human cervical cells: evidence of extensive structural changes during carcinogenesis", *Proceedings of the National Academy of Sciences*, Vol. 88, pp. 10988-10992, 1991.
134. Krafft, C., Neudert, L., Simat, T., Salzer, R., "Near infrared Raman spectra of human brain lipids", *Spectrochimica Acta Part A: Molecular and Biomolecular Spectroscopy*, Vol. 61, pp. 1529-1535, 2005.
135. Thamann, T. J., Lord, R. C., Wang, A. H., Rich, A., "The high salt form of poly (dG-dC): poly (dG-dC) is left-handed Z-DNA: Raman spectra of crystals and solutions", *Nucleic acids research*, Vol. 9, pp. 5443-5458, 1981.
136. Shetty, G., Kendall, C., Shepherd, N., Stone, N., Barr, H., "Raman spectroscopy: elucidation of biochemical changes in carcinogenesis of oesophagus", *British journal of cancer*, Vol. 94, pp. 1460-1464, 2006.

137. Kačuráková, M., Mathlouthi, M., "FTIR and laser-Raman spectra of oligosaccharides in water: characterization of the glycosidic bond", *Carbohydrate Research*, Vol. 284, pp. 145-157, 1996.
138. Samek, O., Jonáš, A., Pilát, Z., Zemánek, P., Nedbal, L., Tříška, J., Kotas, P., Trtílek, M., "Raman microspectroscopy of individual algal cells: sensing unsaturation of storage lipids in vivo", *Sensors*, Vol. 10, pp. 8635-8651, 2010.
139. Cerqueira, M. A., Souza, B. W., Teixeira, J. A., Vicente, A. A., "Effect of glycerol and corn oil on physicochemical properties of polysaccharide films—A comparative study", *Food hydrocolloids*, Vol. 27, pp. 175-184, 2012.
140. Prescott, B., Steinmetz, W., Thomas, G., "Characterization of DNA structures by laser Raman spectroscopy", *Biopolymers*, Vol. 23, pp. 235-256, 1984.
141. Williams, R. W., Dunker, A. K., "Determination of the secondary structure of proteins from the amide I band of the laser Raman spectrum", *Journal of molecular biology*, Vol. 152, pp. 783-813, 1981.
142. Pallant, J., *SPSS survival manual: A step by step guide to data analysis using SPSS*, Open University Press, 2010.